Space Instrumentation
(ELEC-E4220)

Gamma-ray satellites

Fermi Gamma-ray Space Telescope

Talvikki Hovatta

Finnish Centre for Astronomy with ESO

University of Turku / Aalto U.

Outline

- Introduction
- Gamma-ray detection techniques
  - Photoelectric effect
    - GBM instrument
  - Compton scattering
  - Pair production
- Fermi LAT instrument
  - Tracker
  - Calorimeter
- Event analysis
  - From trigger to event reconstruction
- Fermi Science

Introduction

Electromagnetic spectrum

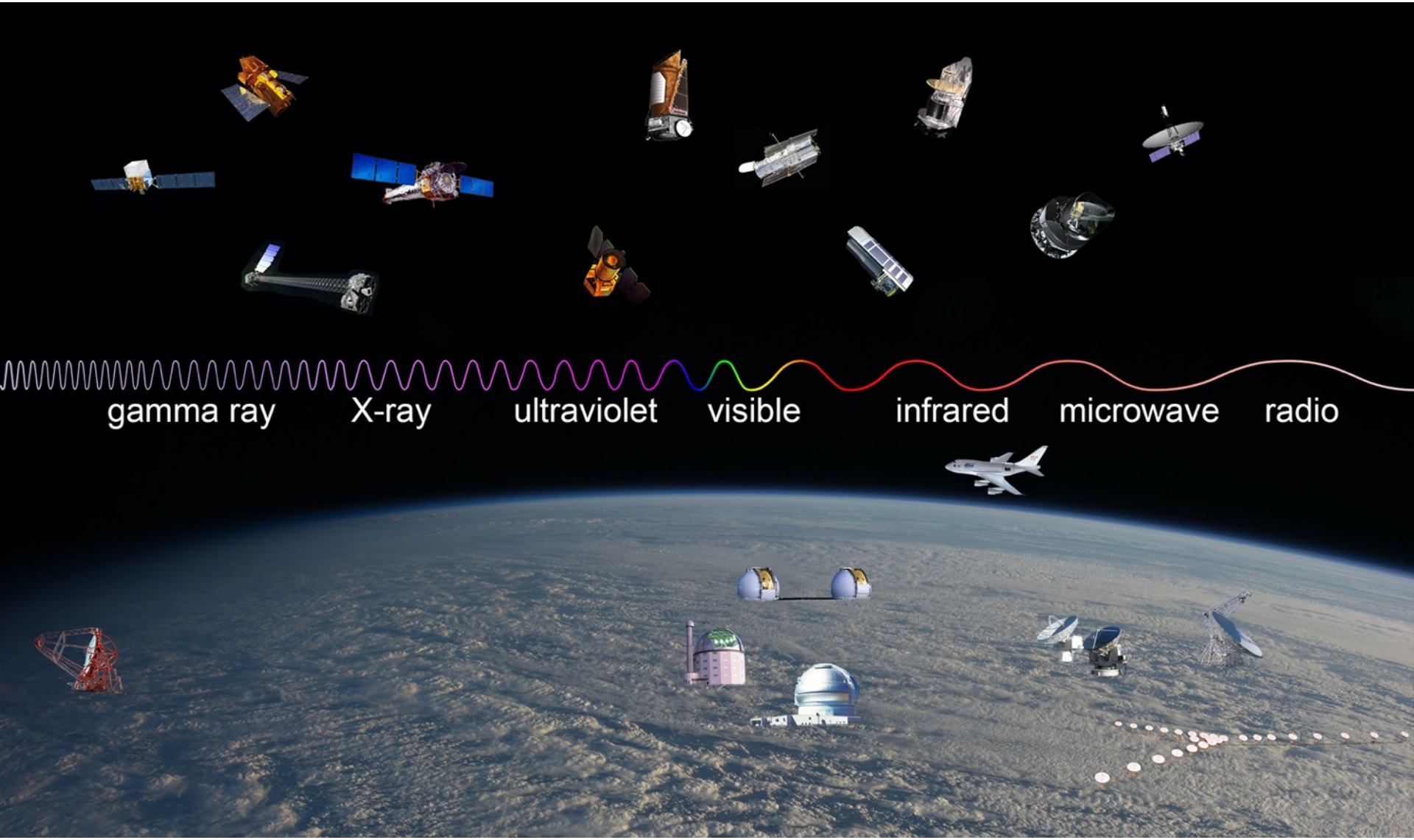

Gamma rays

- $E > 100$ keV, $f > 10^{19}$ Hz, $\lambda < 10^{-11}$m
- In astronomy is high-energy non-thermal emission
  - Emission does not depend on the physical temperature of the object
  - Not necessarily from radioactive decay
- Requires extreme particle acceleration
- Typical emission processes are inverse Compton emission or pion decay

Gamma-ray sky

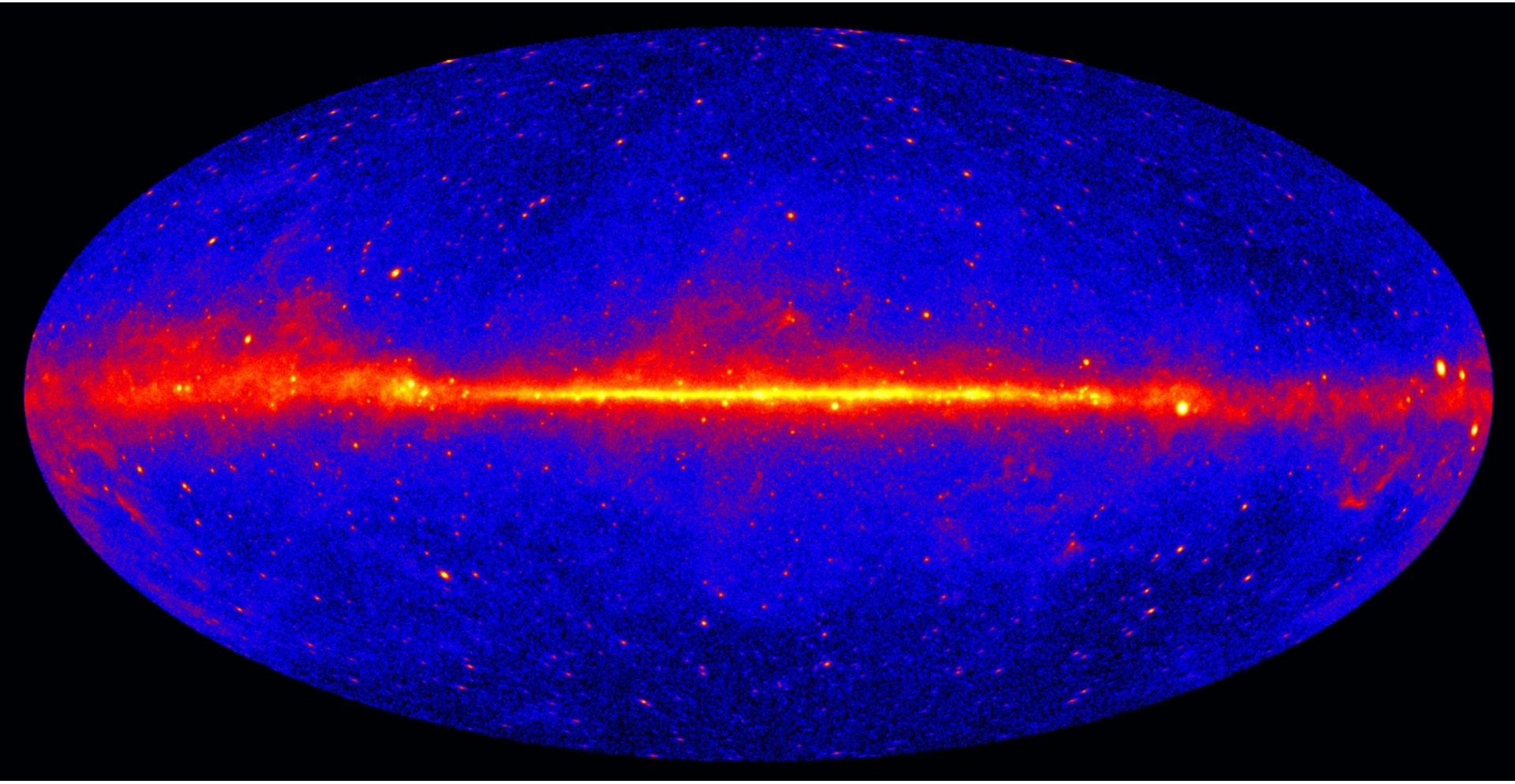

Fermi 5-year sky

Gamma-ray sources in our Galaxy

- Diffuse emission from the plane of the Galaxy
  - From interaction of high energy cosmic rays with interstellar matter
- Supernova remnants
- Pulsars
- Fermi “bubbles”
  - Remnant jet emission?

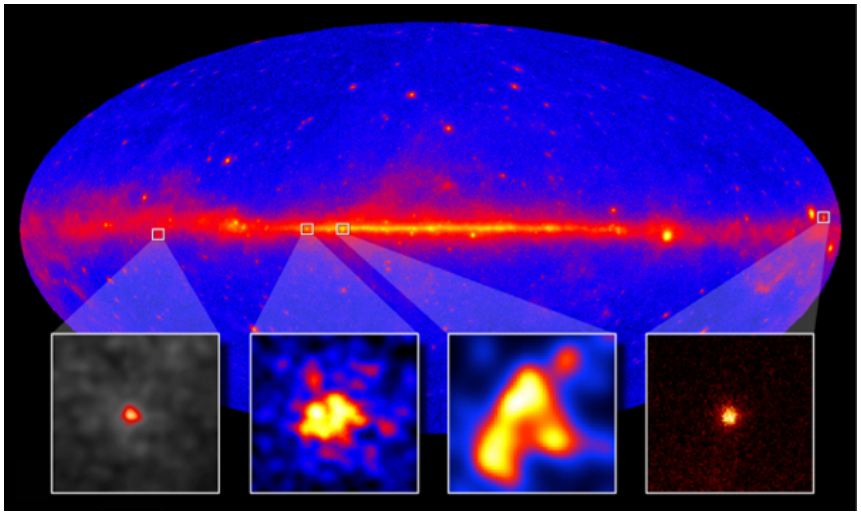

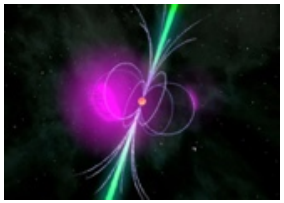

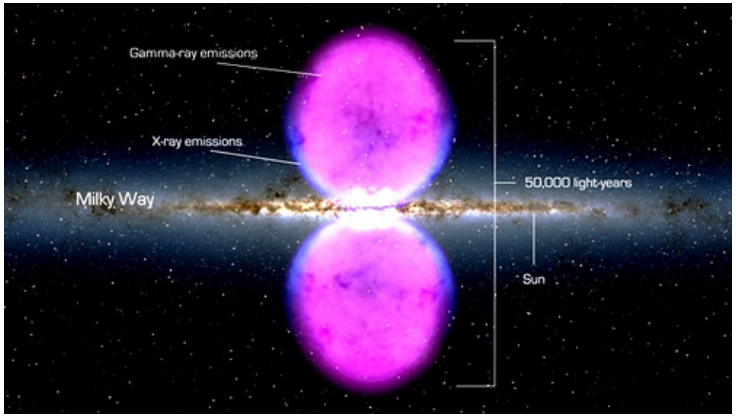

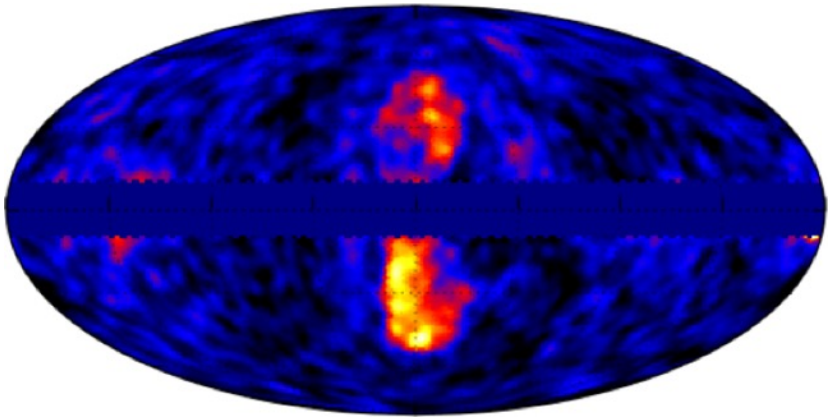

Extragalactic Gamma-Ray sources

- Diffuse emission from unresolved gamma-ray sources
- Active galactic nuclei
- Starburst galaxies
- Gamma-ray bursts
- Merging neutron stars

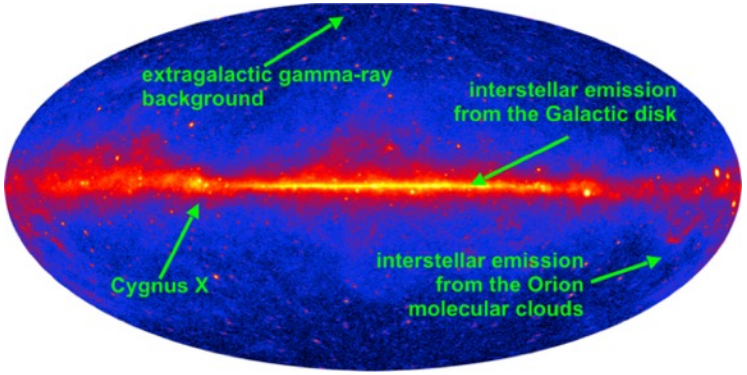

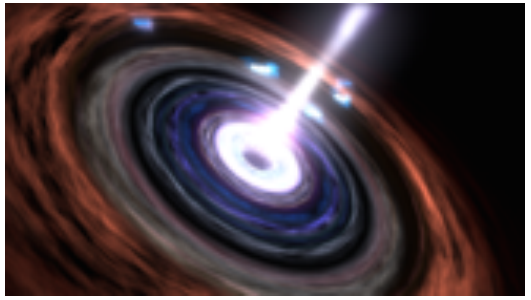

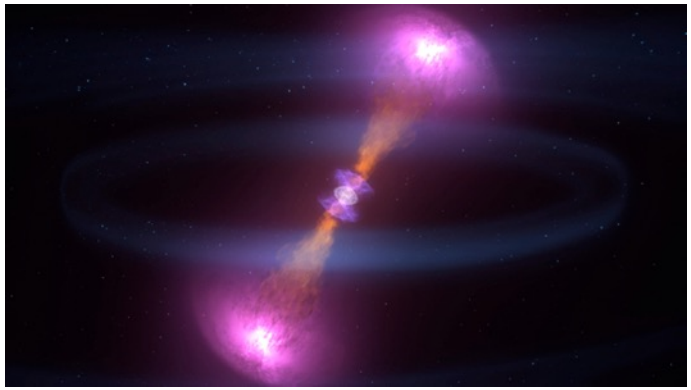

Variable gamma-ray sky

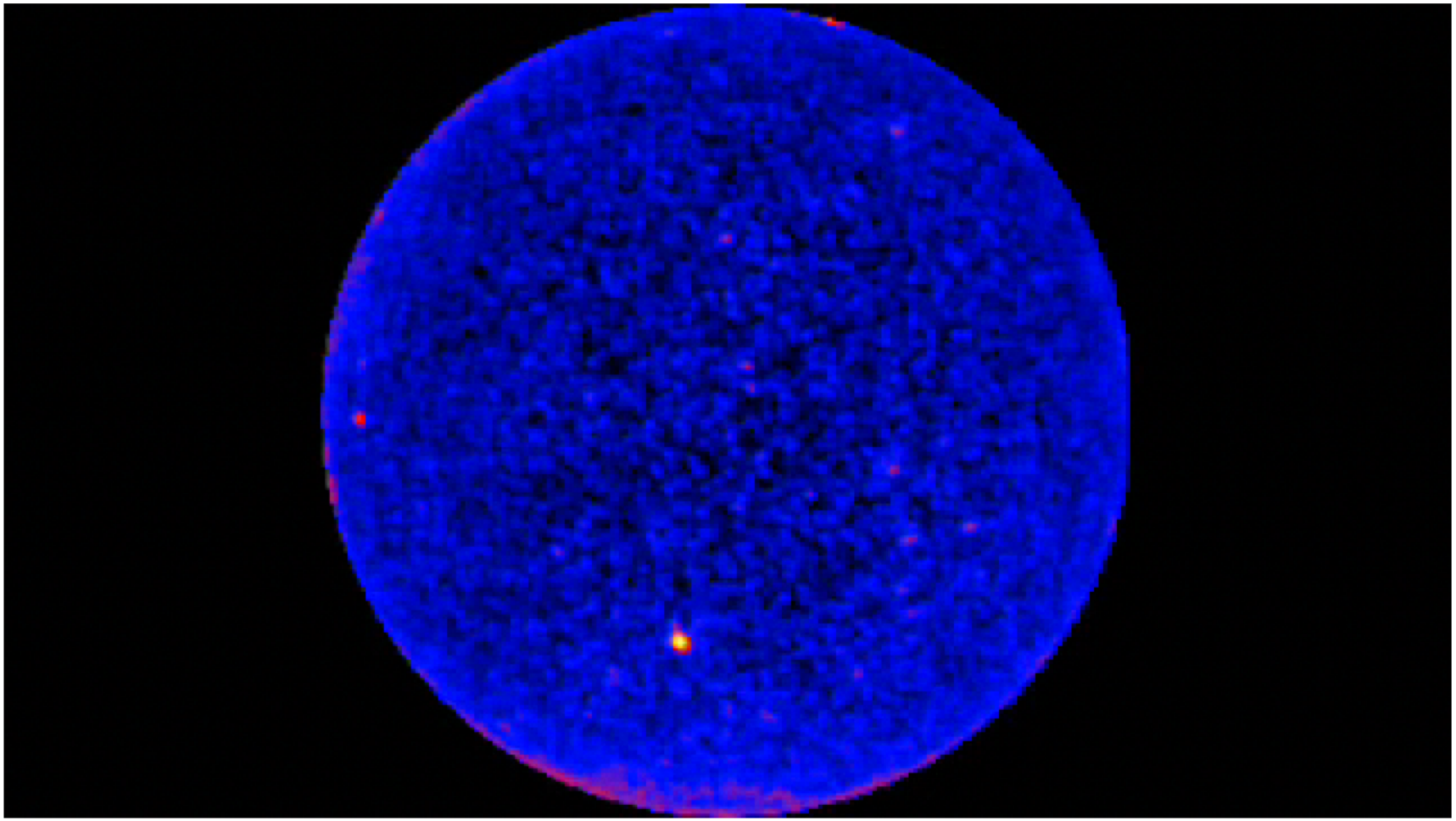

Credit: NASA

Fermi gamma-ray space telescope

- Launched on June 11, 2008
  - Data available since August 2008
- Low Earth orbit at ~565km
- Orbit period 95.33 min
  - Full sky coverage in 2 orbits!
  - Some changes to survey mode due to a solar panel failure in spring 2018
- Planned lifetime 5 years
  - Still on-going
  - No consumables!
- 2 instruments:
  - GBM 8 keV – 40 MeV (GRB detection)
  - LAT 30 MeV – 300 GeV (imaging instrument)

LAT Instrument

(Large Area Telescope under the AntiCoincidence Detector)

Tracker
4 x 4 Array of Towers

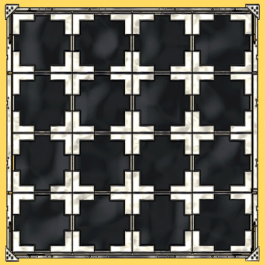

top view

side view

Calorimeter

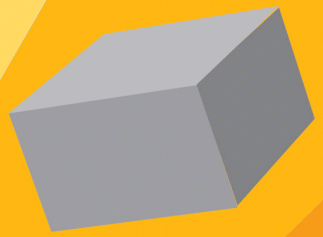

AntiCoincidence
Detector

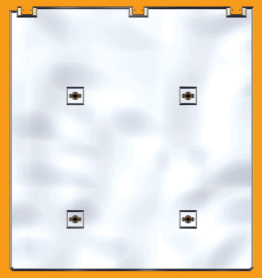

LAT Radiator

Solar Panels

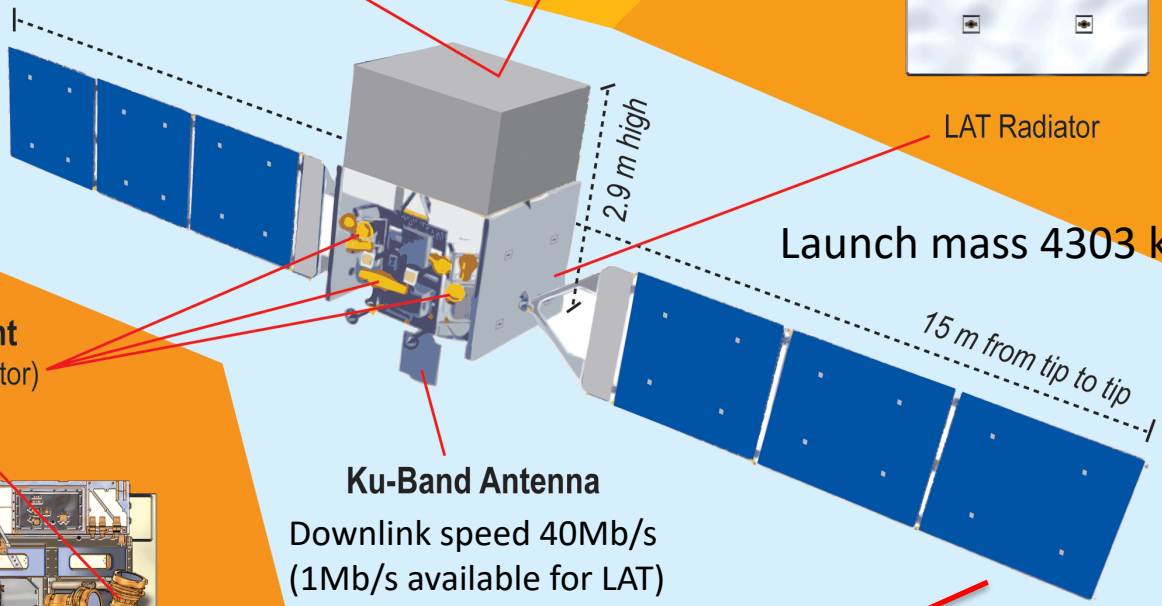

Launch mass 4303 kg

GBM Instrument
(GLAST Burst Monitor)

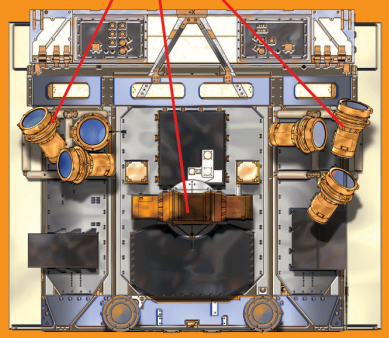

Ku-Band Antenna

Downlink speed 40Mb/s
(1Mb/s available for LAT)

GLAST FERMI

Gamma Ray Large Area Space Telescope

http://www.nasa.gov/glast

Gamma-ray detection techniques

Gamma-ray detection

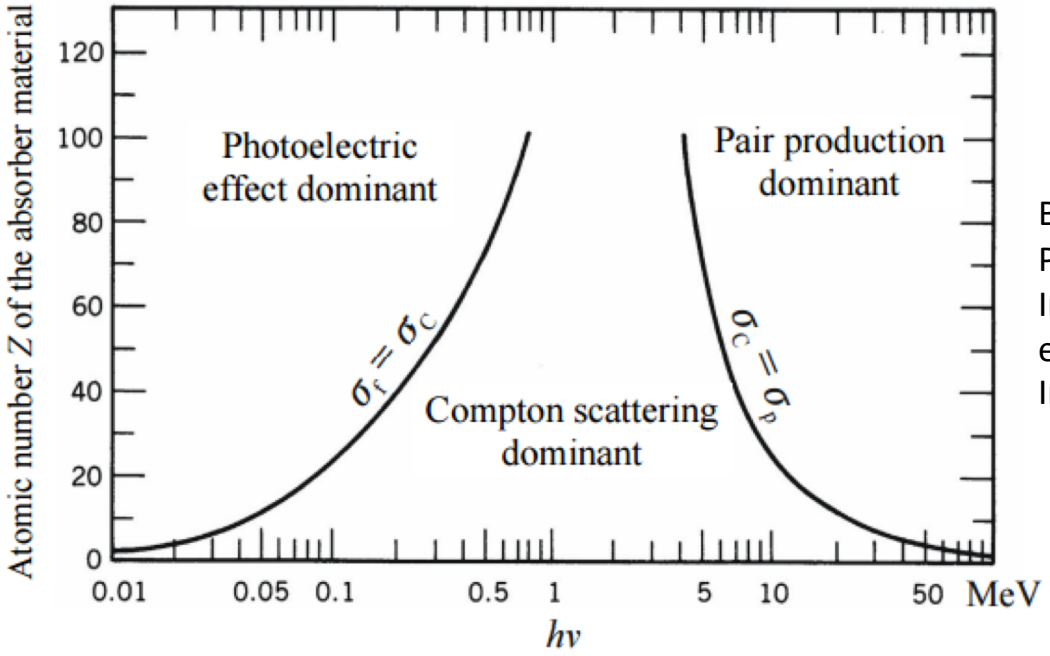

Book: Handbook of Particle Detection and Imaging
edited by Claus Grupen, Irène Buvat.

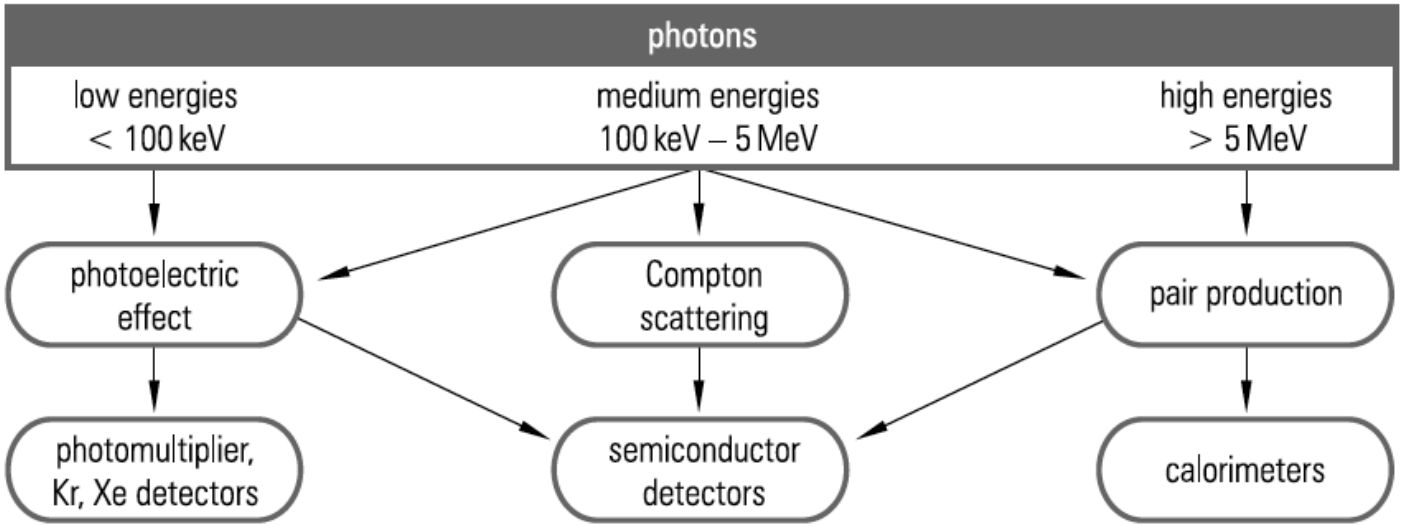

Scintillators

Photoelectric effect (< 100 keV)

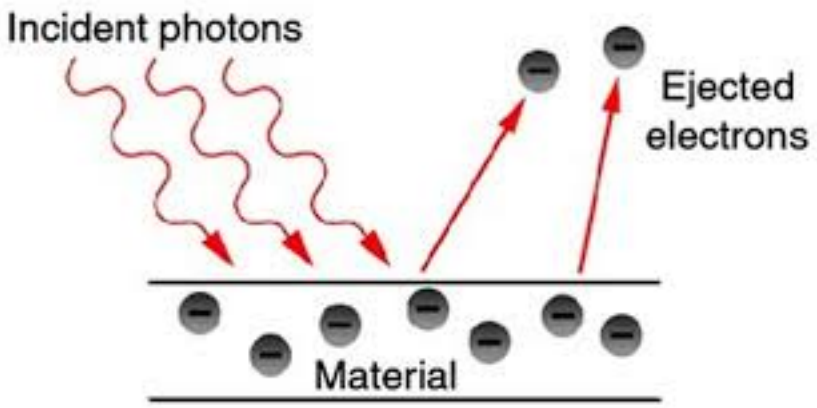

- A photon absorbs into material and gives all its energy to electrons in the absorbing material
- Einstein got a Nobel prize in 1921 for “his discovery of the law of the photoelectric effect"

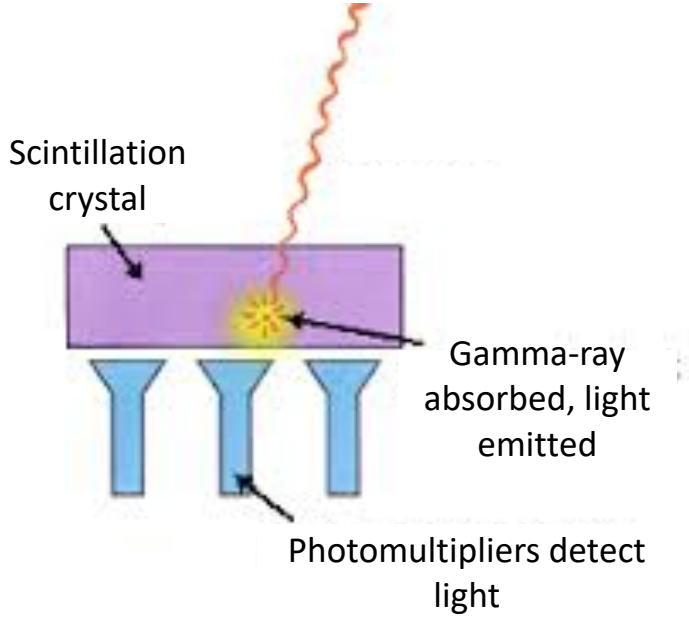

- In gamma-ray instruments a scintillation crystal is used (e.g. NaI or CsI)
- Instead of electrons a light flash is emitted
- Photomultiplier tubes detect the light and convert it to an electrical signal
- Used e.g. in GBM on Fermi and many X-ray satellites

Scintillation

- Scintillator = material that absorbs the energy of an incoming particle
- Scintillates = re-emits the absorbed energy in form of light (low-energy photons)

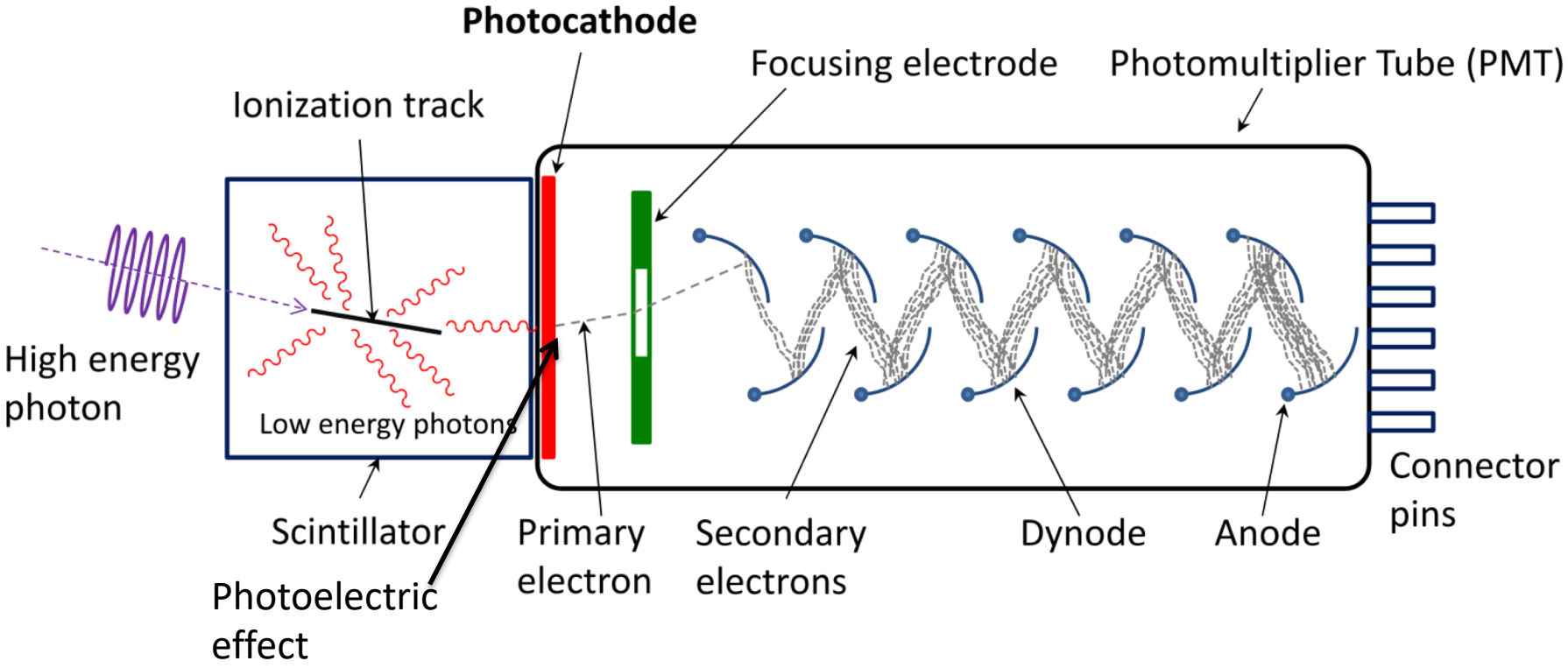

Gamma-ray Burst Monitor (GBM)

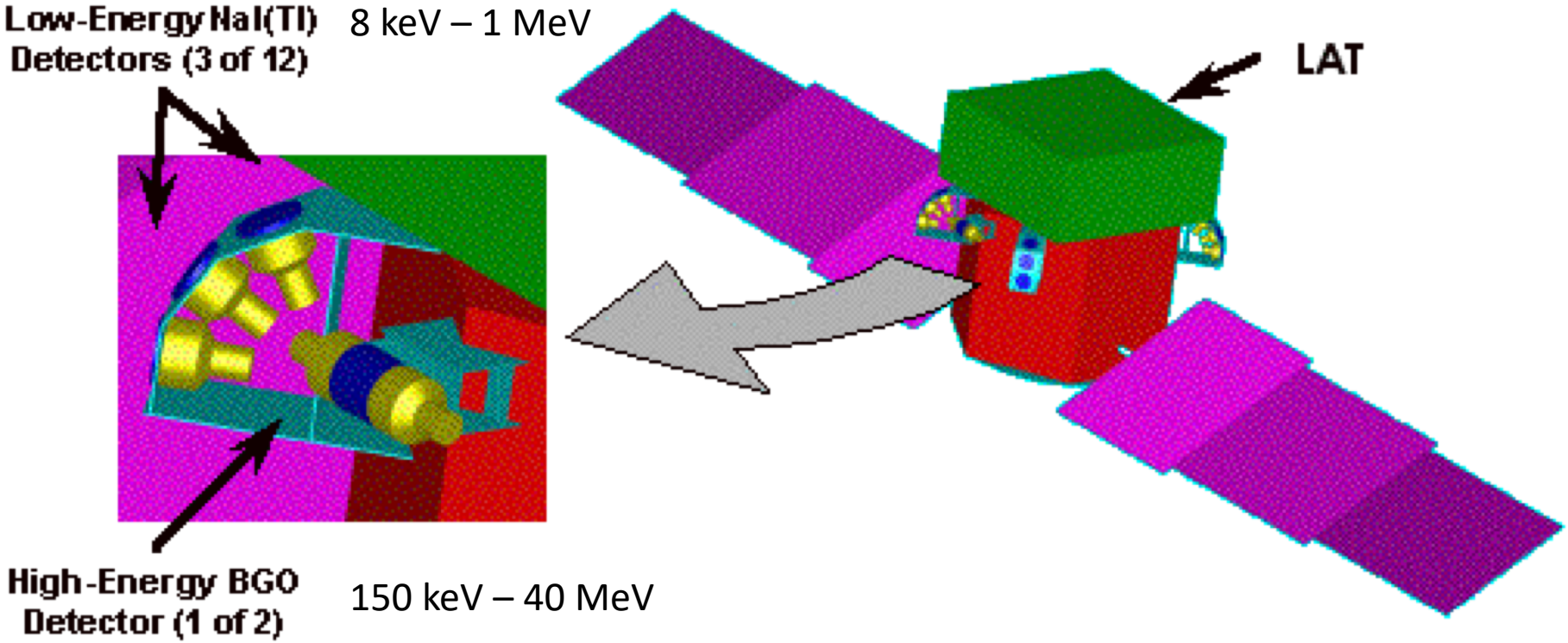

- Nearly full-sky view with detectors placed on opposite sides of the satellite
- Provides a trigger when the photon counts in at least 2 detectors show a significant increase
- Time resolution 2 μs
  - Needed for detection of short GRBs that last < 1s

Compton scattering (100keV-5MeV)

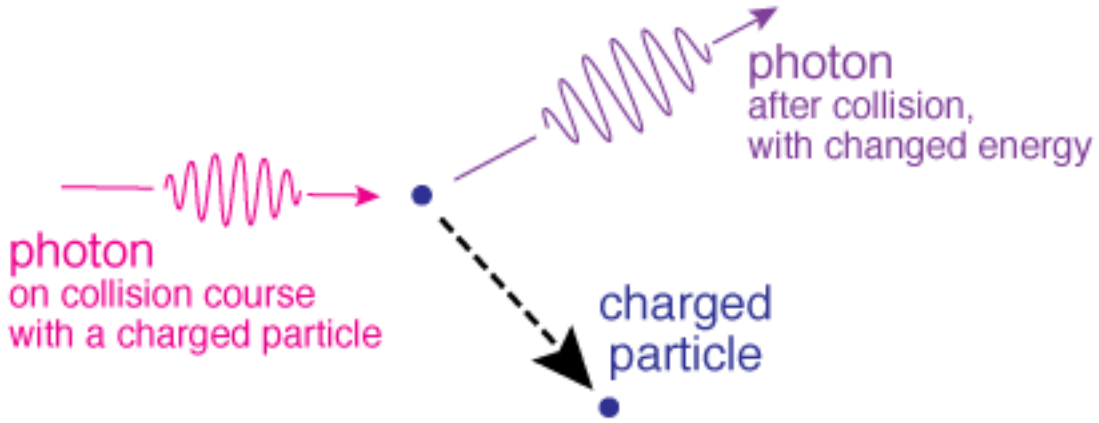

- A photon collides with an electron and gives some of its energy to it

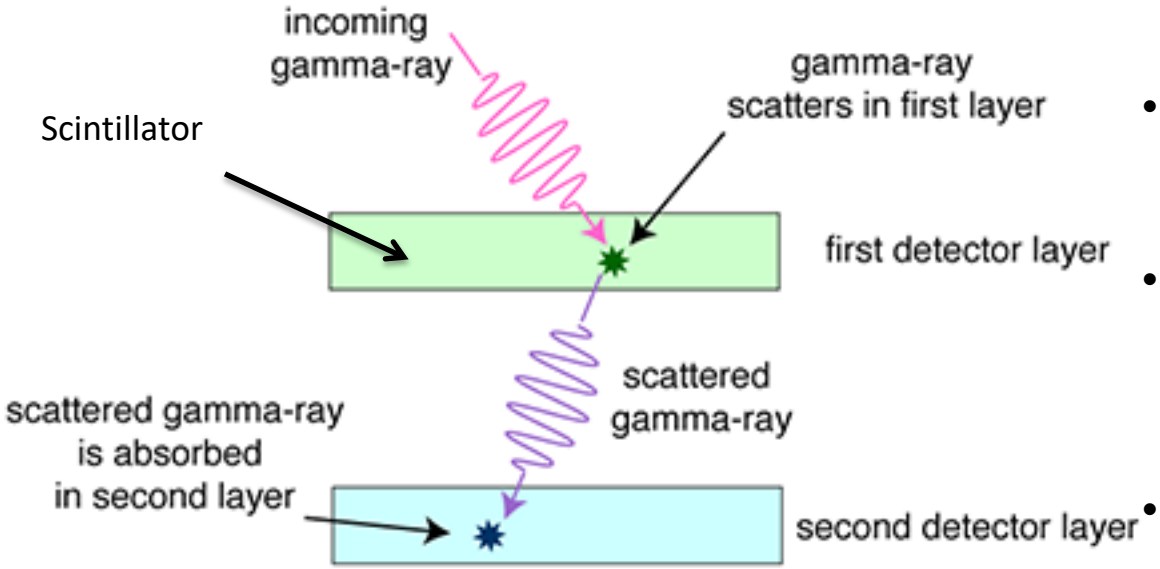

- In gamma-ray instruments the gamma-ray first interacts with a scintillator
- The scattered gamma-ray then gets absorbed in another scintillator that is viewed by phototubes
- Used e.g. in the COMPTEL instrument on board CGRO

Pair production (>5MeV)

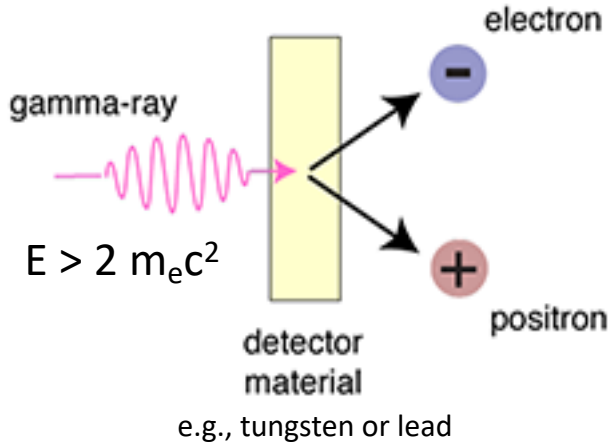

- A photon goes near the nucleus of an atom and gives its energy to an electron-positron pair
- The energy of the photon must be at least two times the rest mass of an electron
  - Dominant mechanism for photons with > 30 MeV energy

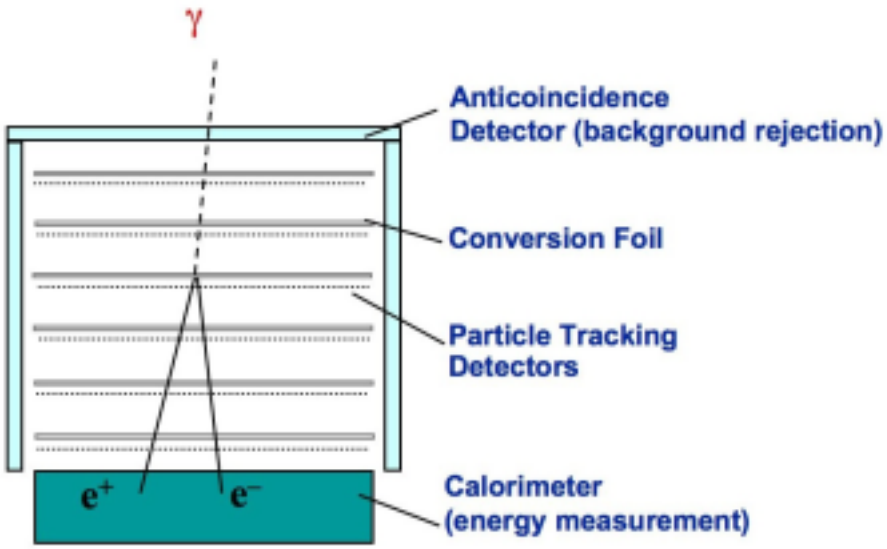

- In gamma-ray instruments there is usually a series of converter foils and tracking material to track the path of the pair
- The energy of the photon is calculated from the pair in a Calorimeter
- Used e.g. in LAT and in its predecessor EGRET

Fermi Large Area Telescope (LAT)

Large Area Telescope (LAT)

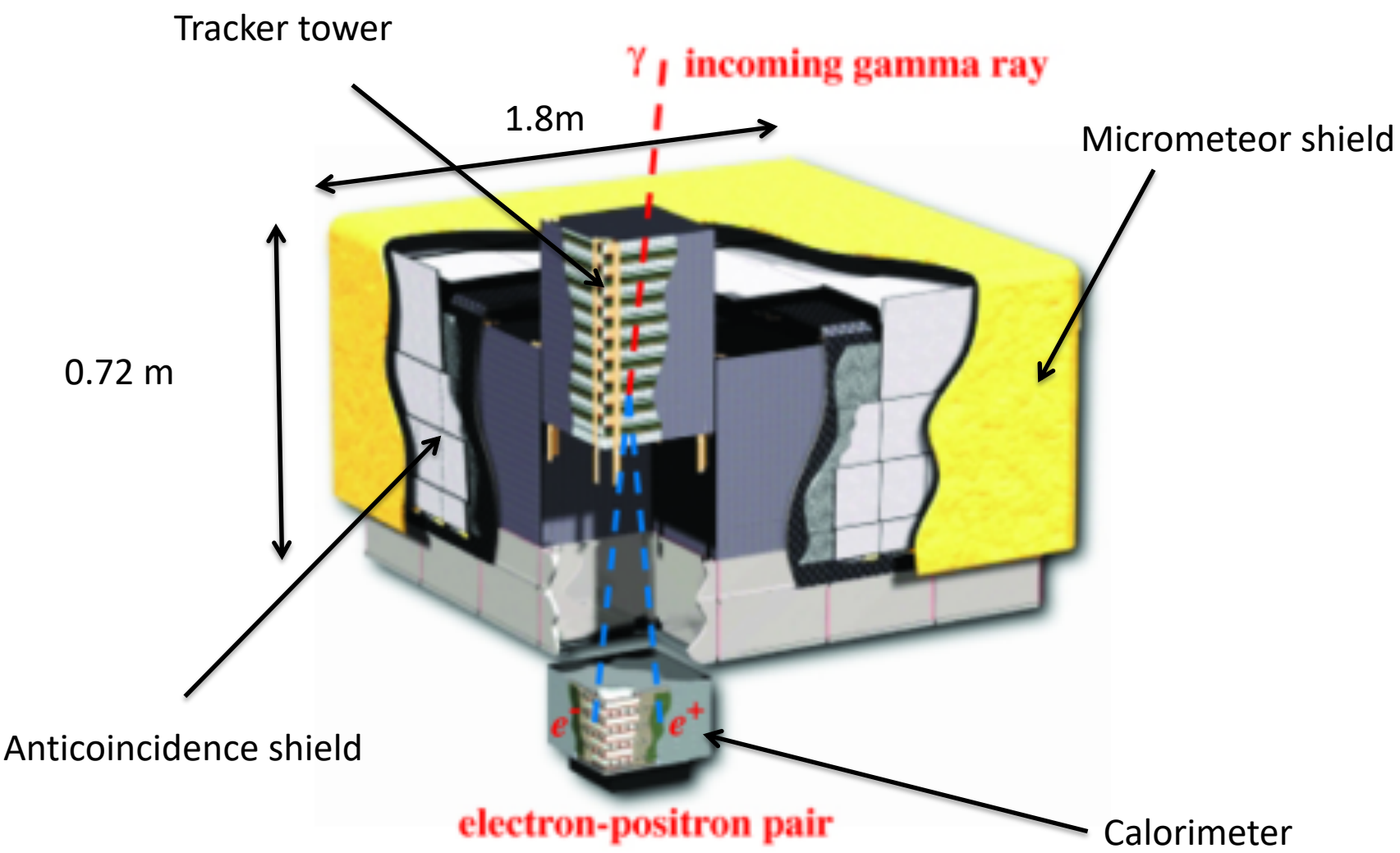

Design considerations

- Size of the “telescope” = size of the detector
  - Field of View of LAT is 2.4 sr (20% of the sky)
- Need a large mass or “radiation length” to absorb the gamma rays
  - Mass of LAT is ~2800 kg, Calorimeter is 1800kg
- Anticoincidence shield is used to discard cosmic rays
  - For each gamma-ray photon there is at least 100 000 Cosmic rays entering the telescope
  - Made of plastic scintillator tiles that are sensitive to charged particles (protons, electrons) but not neutral photons
  - The “trigger” system will discard most of the Cosmic ray events before sending the data down

LAT tracker

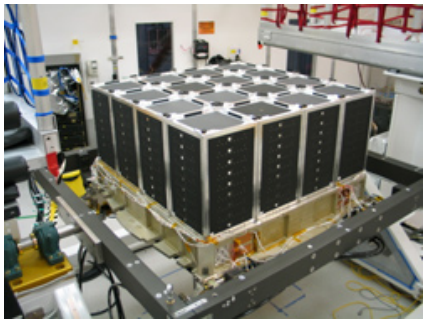

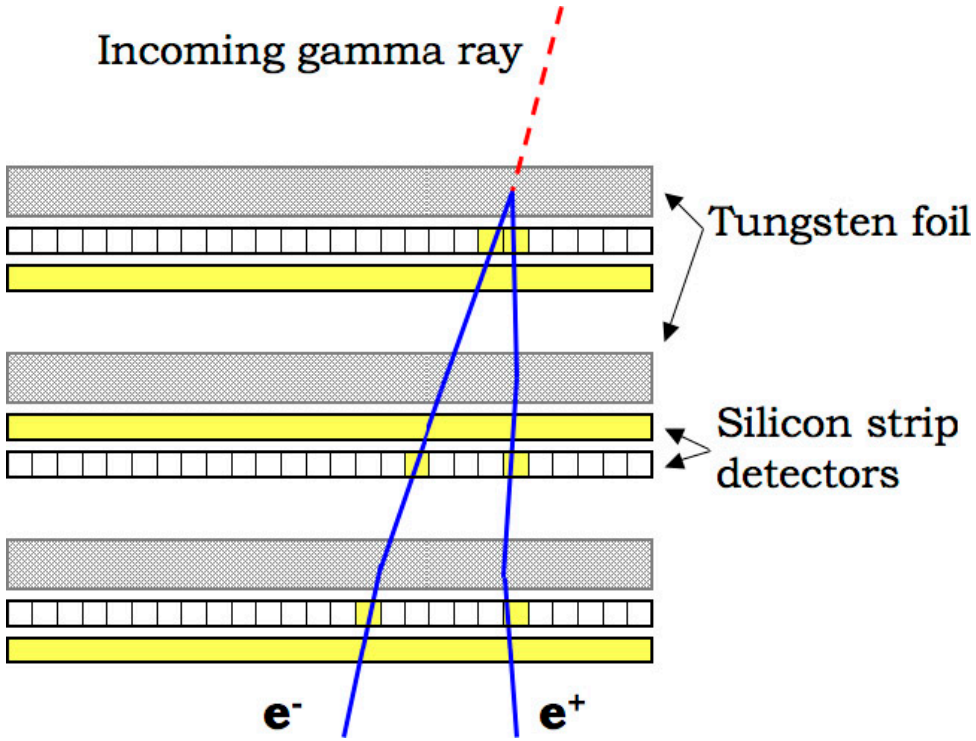

- Gamma-ray photon interacts with tungsten foil where an electron-positron pair is formed
- Silicon strip detectors detect the charged particles and their path can be followed
  - No consumables!
  - Different to EGRET, which used a spark chamber as a tracker
- LAT tracker has 16 planes of tungsten
  - The top 12 foils are thinner (3% radiation length = 0.095mm) than the bottom 4 foils (18% radiation length = 0.72mm) to optimize detection and angular resolution at different energy ranges

Conversion efficiency (how many gamma-rays pair produce) is ~ 63% above 1 GeV

Cosmic ray spark chamber

https://www.youtube.com/watch?v=DpW08xV3RI8

Why silicon strip over spark chamber?

- Only consumable is electricity instead of gas that eventually runs out
- Efficient particle detection in a thin layer
- Reliable once installed
- Power consumption went down in last years
- Price of SSDs went down

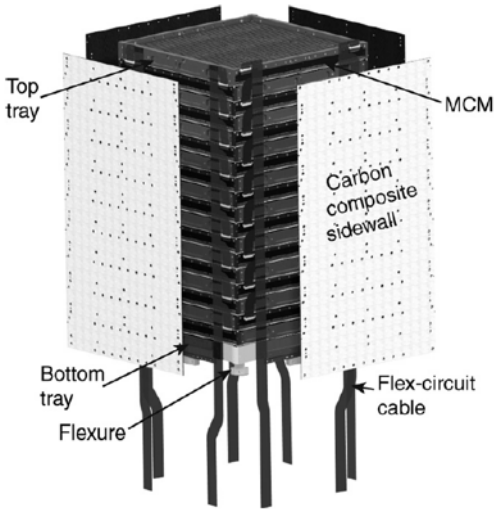

Fig. 2. Exploded view of a Tracker tower module. The detailed cable terminations at the top (Fig. 11) have been omitted from this drawing.

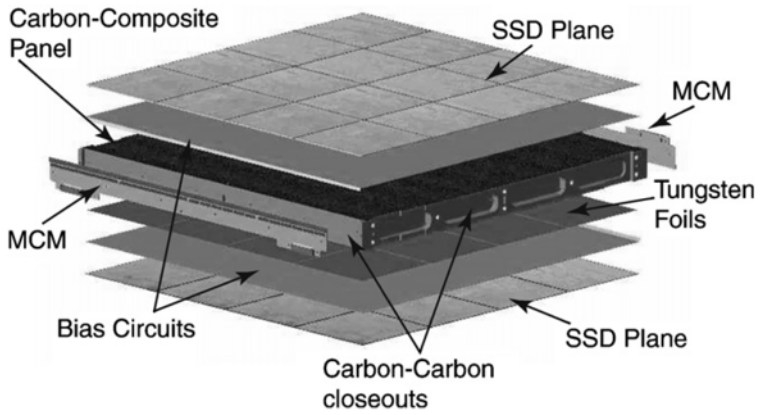

Fig. 5. Exploded view of a mid tray, illustrating the integration of detectors and electronics.

- Each tower has 576 SSDs
- Multi-chip-modules (MCM) read them out

Atwood et al. 2007 https://doi.org/10.1016/j.astropartphys.2007.08.010

LAT Calorimeter

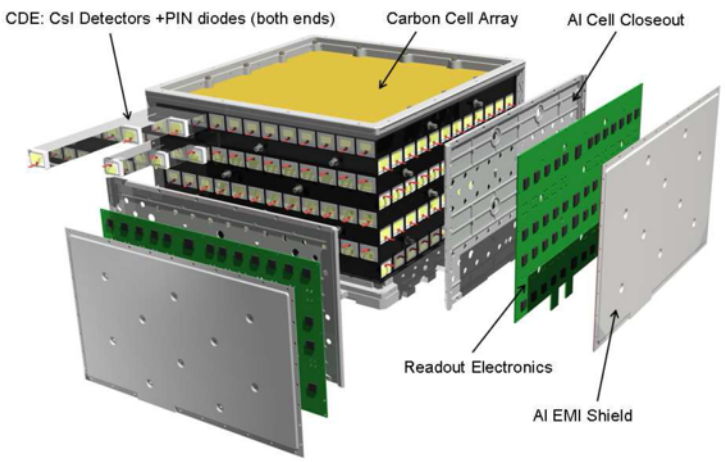

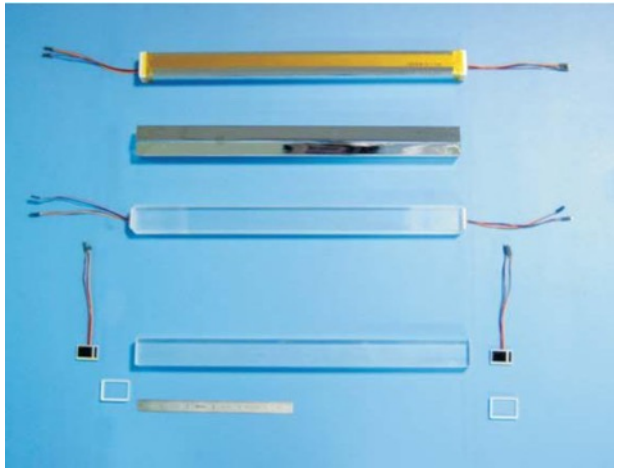

- 4x4 array in the bottom of the tracker
- The incoming electron-positron pair gets fully absorbed in the calorimeter
- Each calorimeter unit consists of CsI(Tl) crystal detectors in a 12 x 8 hodoscopic array
- The electrons / positrons interact with the crystal detector producing a light flash in gamma-ray energies (photoelectric effect) proportional to the energy deposited
- PIN photodiodes read the scintillating light
  - Each end of the crystal have two photodiodes sensitive to different energy ranges (2 MeV-1.6 GeV and 100 MeV-70 GeV)
  - No need for a photomultiplier because the light yield of CsI crystal is larger than e.g. NaI, which requires PMTs

Localization within each crystal

- Location of the event is provided by the location of the crystal in the calorimeter and the light asymmetry measured at the diodes in the opposite ends of the crystal

- Energy of the event is reconstructed from the amount of light measured at the diodes

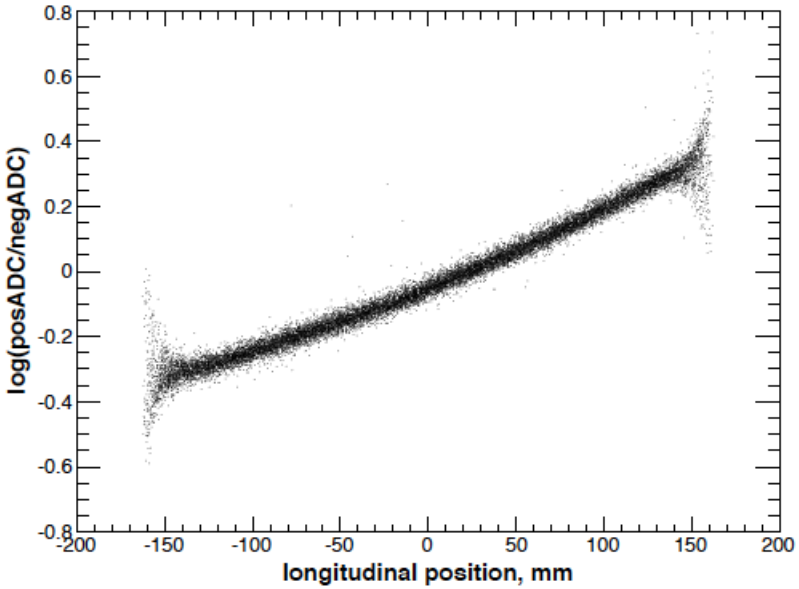

Atwood et al. 2009

FIG. 7.— Light asymmetry measured in a typical calorimeter crystal using sea level muons. The light asymmetry is defined as the logarithm of the ratio of the outputs of the diodes at opposite ends of the crystal. The width of the distribution at each position is attributable to the light collection statistics at each end of the crystal for the ~11 MeV energy depositions of vertically incident muons used in the analysis. This width scales with energy deposition as $E^{-1/2}$.

LAT event reconstruction

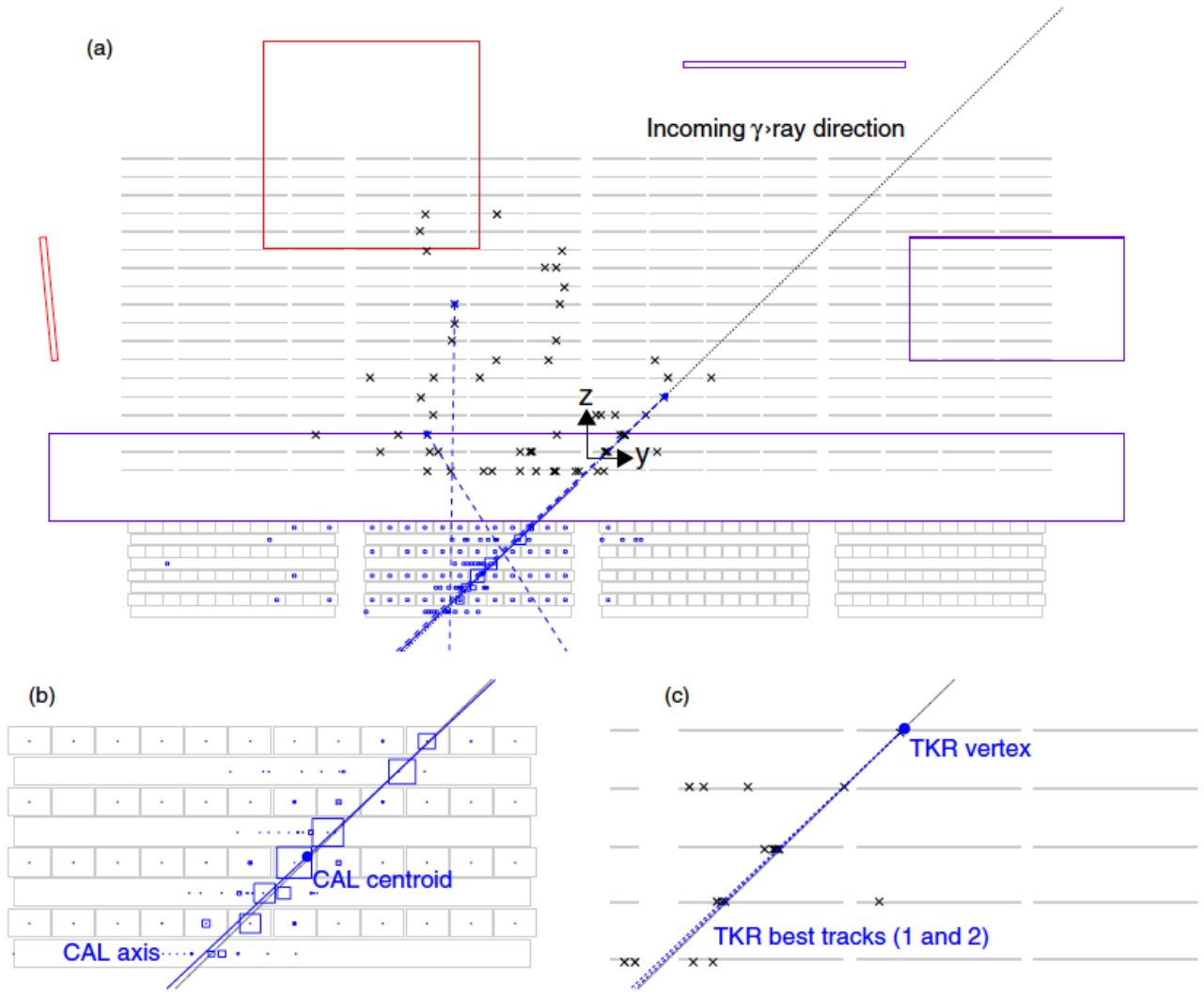

Figure 12. Event display of a simulated 27 GeV γ ray (a) and zoom over the CAL (b) and TKR (c) portions of the event. The small crosses represent the clusters in the TKR, while the variable-size squares indicate the reconstructed location and magnitude of the energy deposition for every hit crystal in the CAL. The dotted line represents the true γ-ray direction, the solid line is the CAL axis (Section 3.2.1), and the dashed lines are the reconstructed TKR tracks (Section 3.2.1). The backsplash from the CAL generates tens of hits in the TKR, with two spurious tracks reconstructed in addition to the two associated with the γ ray (note that they extrapolate away from the CAL centroid and do not match the CAL direction). It also generates a few hits in the ACD, which, however, are away from the vertex direction extrapolation and therefore do not compromise our ability to correctly classify the event as a γ ray.

Event analysis

Hardware is just a small part of the system!

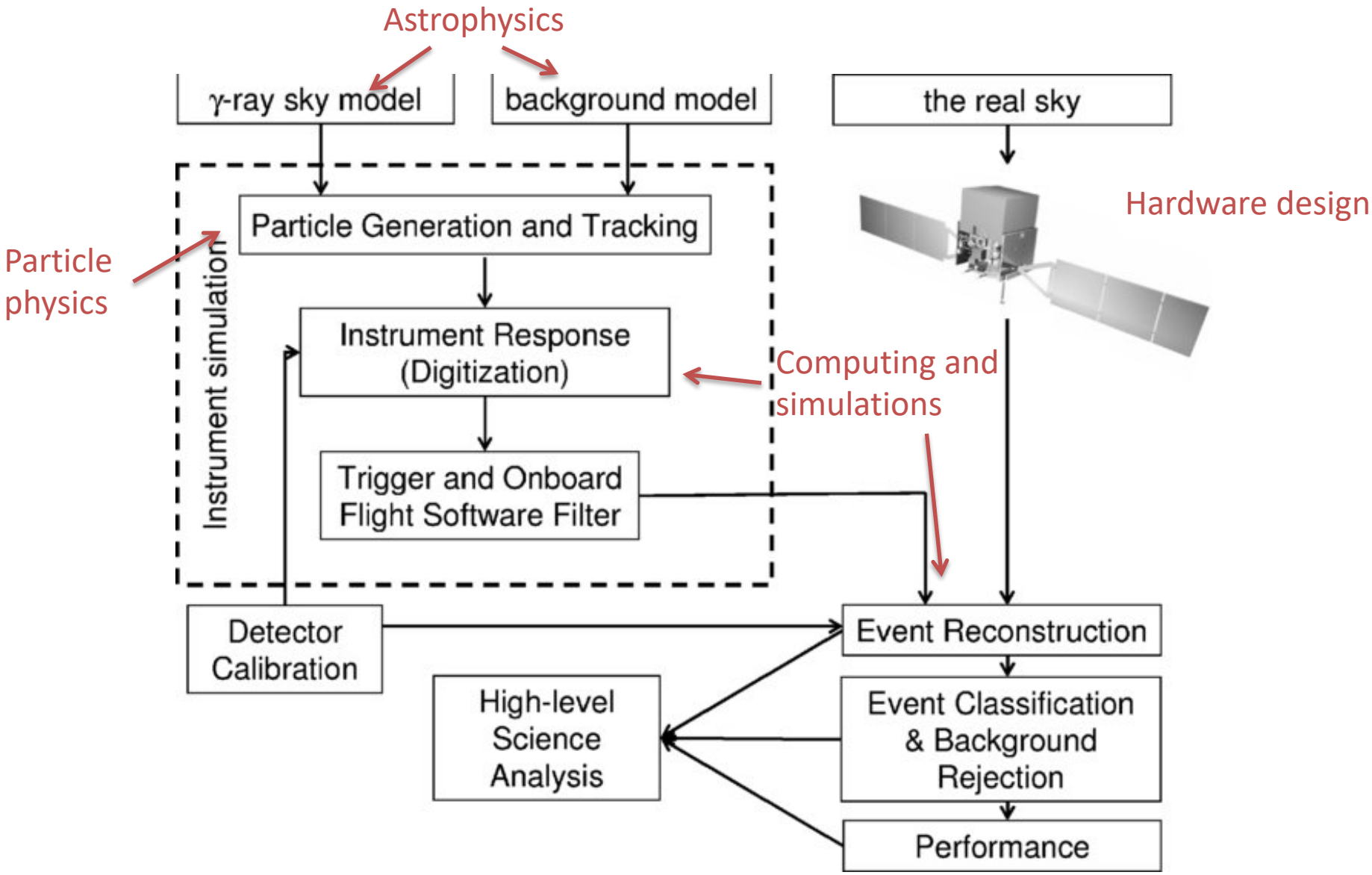

LAT on-board data acquisition system

- Collects data from other subsystems
- Implements multilevel event trigger
- Provides on-board processing to reduce downlinked events (1 photon / 100 000 CR)
  - Also to minimize dead-time from reading out the LAT events
- Performs on-board science analysis to provide triggers for rapid transients (e.g. gamma-ray burst alerts)

Event analysis logical structure

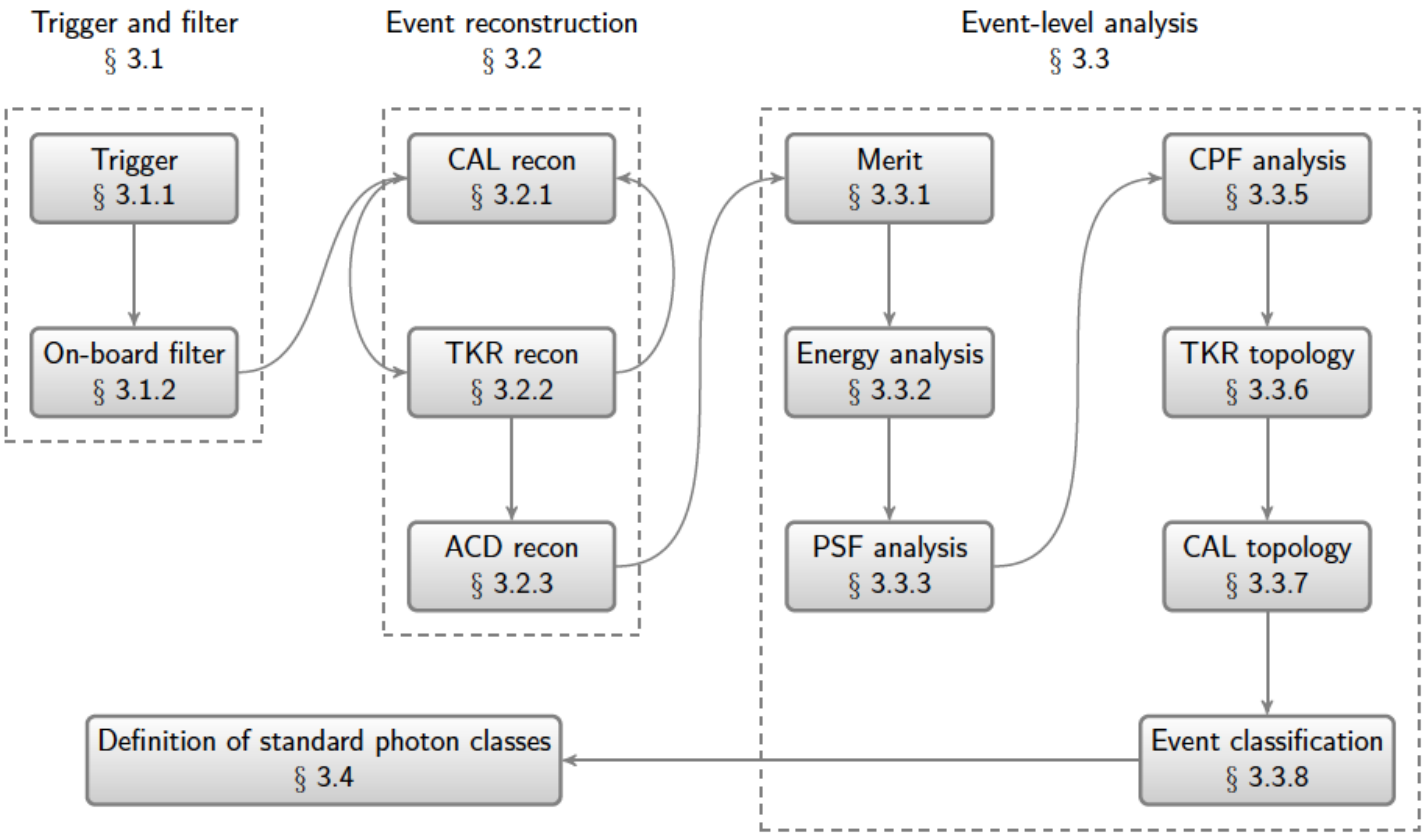

Figure 11. Logical structure of the analysis steps determining which events are selected for a given class. The references to section numbers are meant to help the reader navigate the content of Section 3.

Trigger rates

Event classification

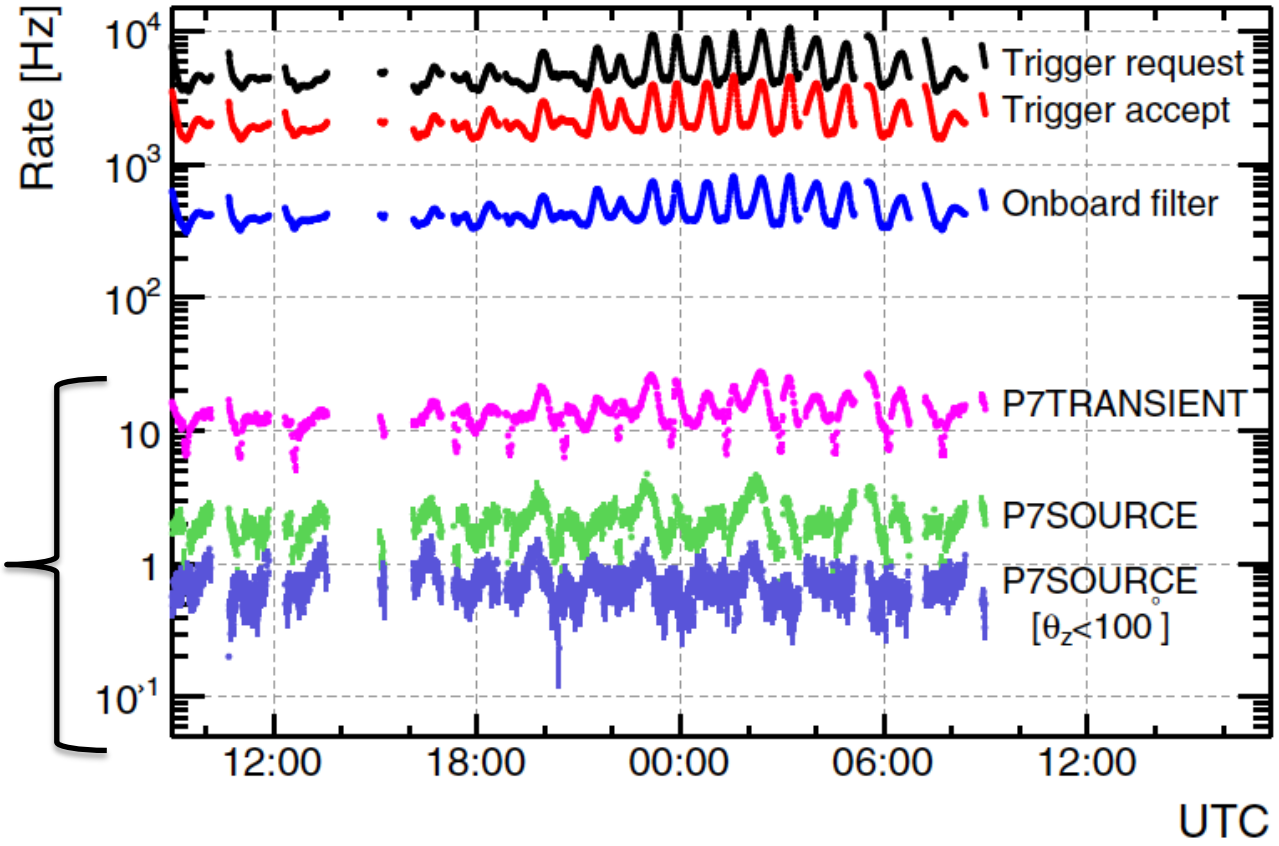

Figure 7. Rates at several stages of the data acquisition and reduction process on a typical day (2011 August 17). Starting from the highest, the curves shown are for the rates (1) at the input of the hardware trigger process (trigger request), (2) at the output of the hardware trigger (trigger accept), (3) at the output of the on-board filter, (4) after the loose `P7TRANSIENT` γ-ray selection, (5) after the tighter `P7SOURCE` γ-ray selection, and (6) the `P7SOURCE` γ-ray selection with an additional cut on the zenith angle ($\theta_z < 100°$). See Section 3 for more details about the event selection stages.

LAT trigger and event reconstruction

VETO is issued if any of the ACD tiles react above a certain threshold = main information used in on-board filtering, combined with information from CAL and TRK

Event reconstruction done using pattern recognition algorithms

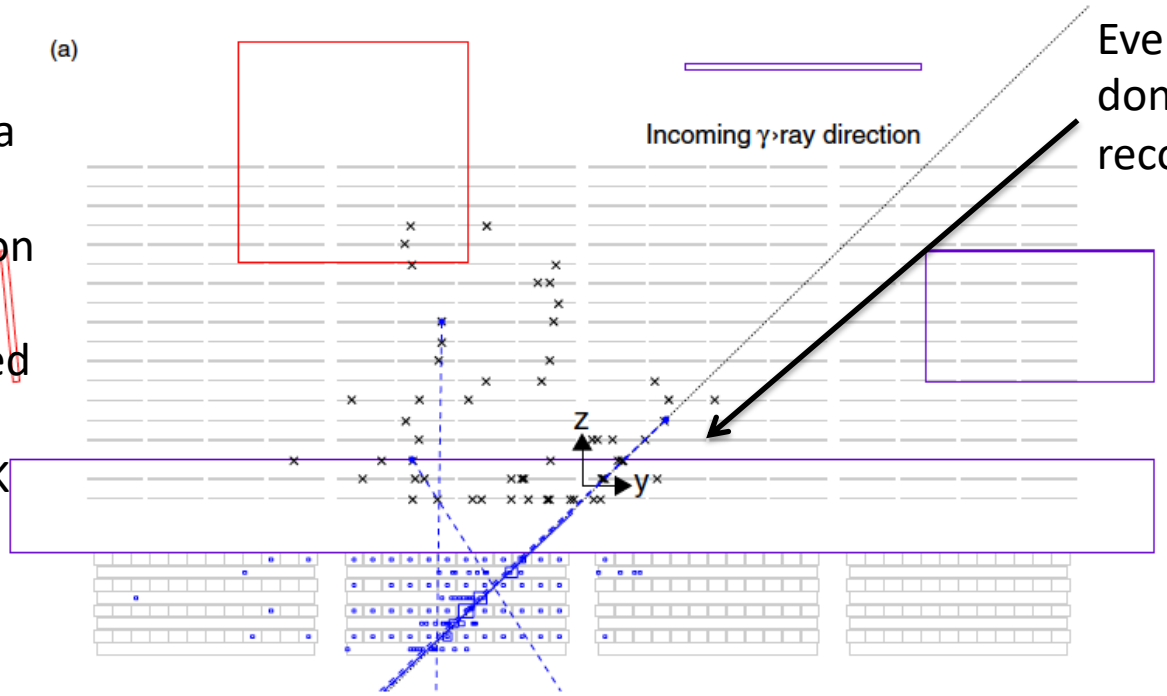

CAL is triggered If any of the crystals show an event with energy above the threshold of the PIN diode

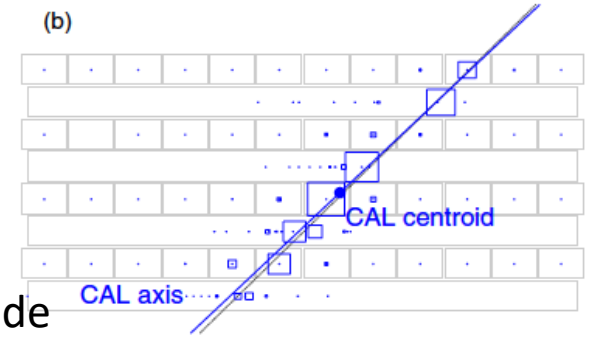

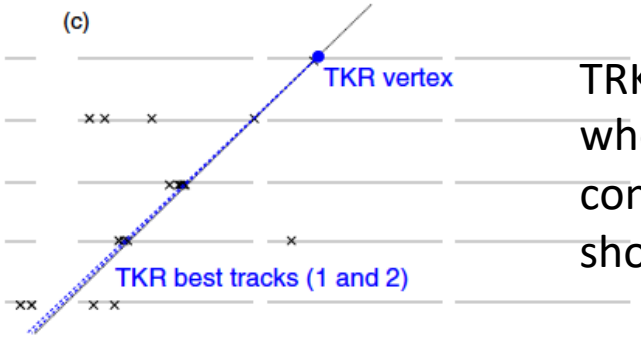

TRK is triggered when at least 3 consecutive layers show an event

Figure 12. Event display of a simulated 27 GeV γ ray (a) and zoom over the CAL (b) and TKR (c) portions of the event. The small crosses represent the clusters in the TKR, while the variable-size squares indicate the reconstructed location and magnitude of the energy deposition for every hit crystal in the CAL. The dotted line represents the true γ-ray direction, the solid line is the CAL axis (Section 3.2.1), and the dashed lines are the reconstructed TKR tracks (Section 3.2.1). The backsplash from the CAL generates tens of hits in the TKR, with two spurious tracks reconstructed in addition to the two associated with the γ ray (note that they extrapolate away from the CAL centroid and do not match the CAL direction). It also generates a few hits in the ACD, which, however, are away from the vertex direction extrapolation and therefore do not compromise our ability to correctly classify the event as a γ ray.

LAT event analysis

1. Selects the best candidate track
2. Calculates the most likely energy for the event
3. Chooses the best direction for the event
4. Performs charged particle rejection
5. Flags likely cosmic rays (CRs) based on tracker signal
6. Flags CRs based on calorimeter signal
7. Estimates the gamma-ray probability and classifies the event (e.g. transient or source)

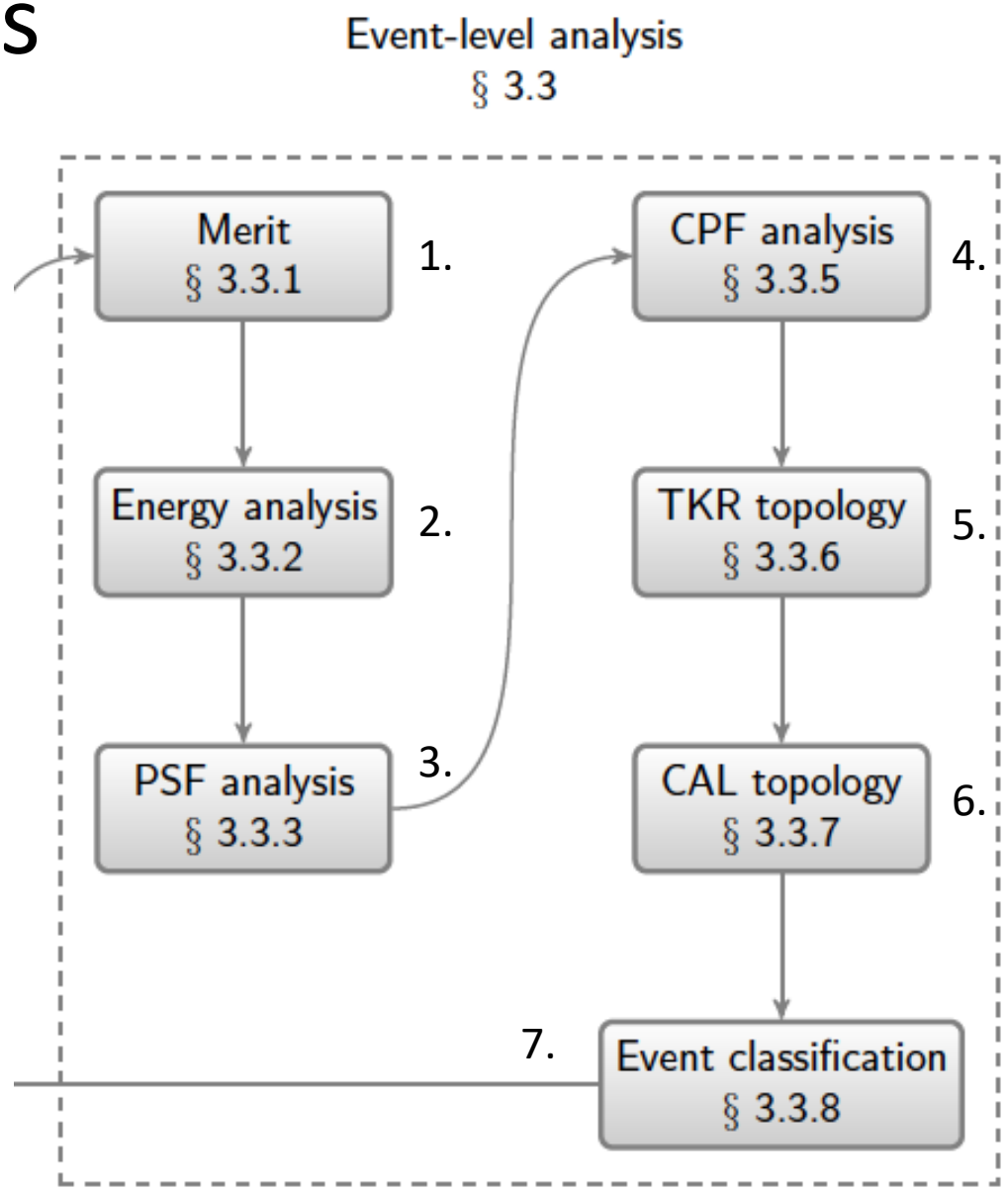

Instrument response functions (IRFs)

- Describe the instrument performance
  - Effective area, point-spread function, energy dispersion as a function of energy
  - Monte-Carlo simulations on how particles interact with the detectors
- Generated using Maximum likelihood analysis
  - Initial model based on EGRET (Pass 6)
  - Updated based on in-flight experience (Pass 7 and Pass 8)

LAT angular resolution

- Determined by the Point-spread function (PSF)
- PSF = the probability distribution for the reconstructed direction of incident gamma-rays from a point source
- Energy dependent
  - 5^o at 100 MeV
  - 0.2^o at > 20 GeV
  - At low energies dominated by multiple scatterings in the tracker
- Compare to e.g. optical telescopes with angular resolution of ~ 1”

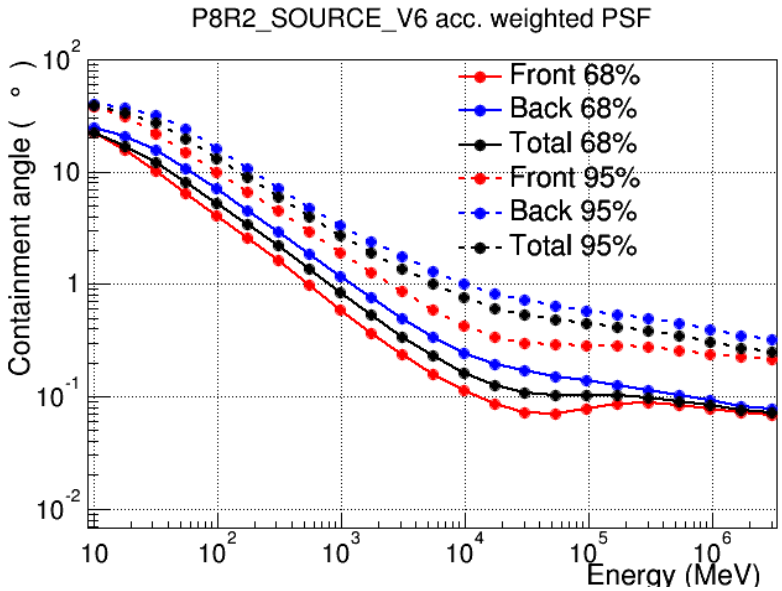

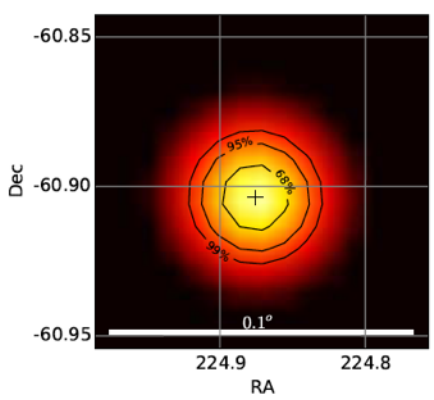

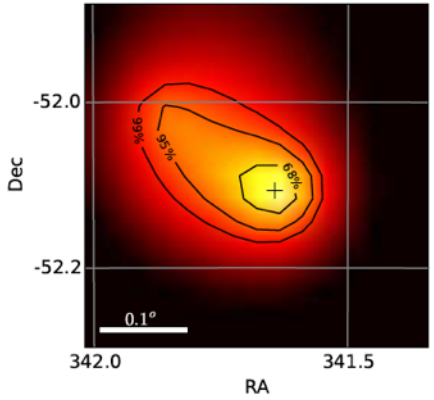

Fermi science

National Aeronautics and Space Administration

Fermi's Decade of Gamma-ray Discoveries

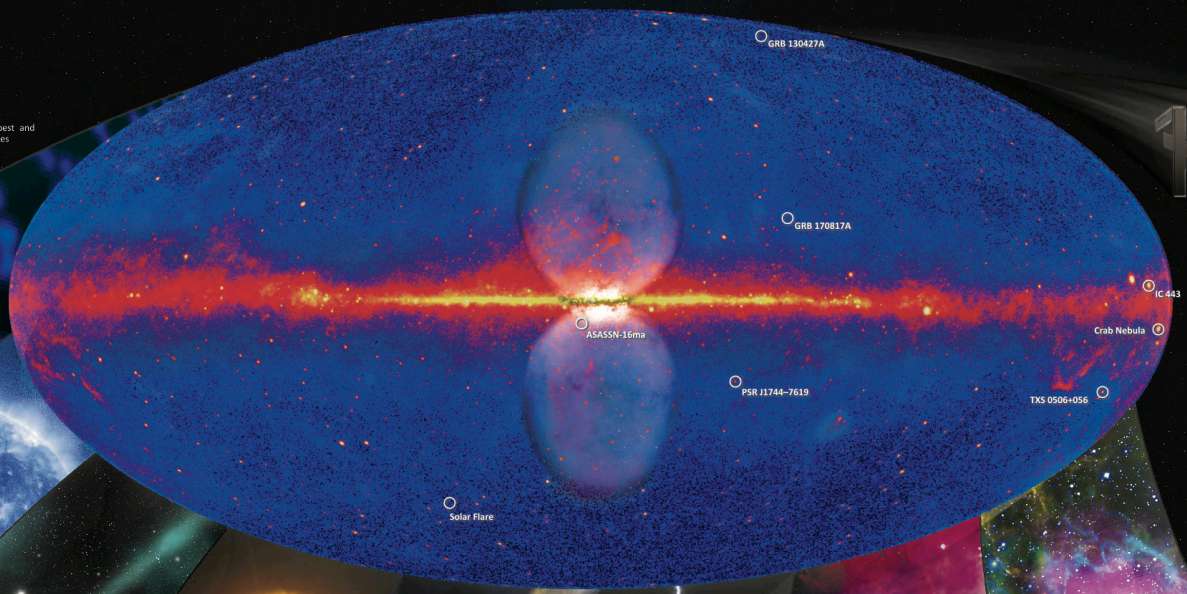

10 years

Fermi 10-year Sky Map

This all-sky view, centered on our Milky Way galaxy, is the deepest and best-resolved portrait of the gamma-ray sky to date. It incorporates observations by NASA's Fermi Gamma-ray Space Telescope from August 2008 to August 2018 at energies greater than 1 billion electron volts (GeV). For comparison, the energy of visible light falls between 2 and 3 electron volts. Lighter shades indicate stronger emission.
NASA/DOE/Fermi LAT Collaboration

GRB 130427A

On April 27, 2013, a blast of light from a dying star in a distant galaxy became the focus of astronomers around the world. The explosion, known as a gamma-ray burst and designated GRB 130427A, was detected by Fermi for about 20 hours. The burst included a 95 GeV gamma ray, the most energetic light yet detected from a GRB.
NASA/DOE/Fermi LAT Collaboration

Solar Flare

Although our Sun is not usually a bright gamma-ray source, solar flares can briefly outshine everything else in the gamma-ray sky. On March 7, 2012, Fermi detected flares erupting on the side of the Sun not visible to the spacecraft. The flares produced accelerated particles that fell onto the side of the Sun facing Earth, resulting in gamma rays Fermi could detect.
NASA/SDO

PSR J1744-7619

Discovered by Einstein@Home, a distributed computing project that analyzes Fermi data using home computers, PSR J1744-7619 is the first gamma-ray millisecond pulsar that has no detectable radio emission.
NASA/DOE/Fermi LAT Collaboration/SSU/R.Simonnet

ASASSN-16ma

Fermi has discovered several novas, outbursts powered by thermonuclear eruptions on white dwarf stars. This was a surprise because novas weren't expected to be powerful enough to produce gamma rays. One event, dubbed ASASSN-16ma, shows that both gamma rays and visible light seem to be produced by the same physical process. *NASA/DOE/Fermi LAT Collaboration*

GRB 170817A

This landmark event represents the first time light was seen from a source that produced gravitational waves. Fermi's detection of GRB 170817A coincided with a signal from merging neutron stars detected by the LIGO and Virgo gravitational-wave observatories. *NSF/LIGO/SSU/A. Simonnet*

TXS 0506+056

Among the nearly 2,000 active galaxies Fermi monitors, TXS 0506+056 stands out as the first one known to have produced a high-energy neutrino. Neutrinos are tiny, ghost-like particles that barely interact with matter and are thought to be produced in the same extreme physical environments as gamma rays. In July 2018, Fermi linked this galaxy to a detection by the Ice Cube Neutrino Observatory at the South Pole.
NASA/Goddard/Fermi LAT Collaboration

Crab Nebula

The Crab Nebula, a young supernova remnant containing a pulsar, surprised Fermi astronomers with gamma-ray flares driven by the most energetic particles ever traced to a specific astronomical object. To account for the flares, scientists say electrons near the pulsar must be accelerated to energies a thousand trillion (10^{15}) times greater than visible light.
NASA/CXC/NDT/ASU/J. Hester et al

Fermi Bubbles

Fermi data revealed vast gamma-ray bubbles extending tens of thousands of light-years From the Milky Way's plane. The Fermi Bubbles may be related to past activity of the supermassive black hole at our galaxy's heart.
NASA Goddard

Galactic Center

The central region of the Milky Way is brighter in gamma rays than expected. Whether this excess is a collection of undiscovered millisecond pulsars or possibly evidence of annihilation of dark matter particles remains a mystery and will be part of Fermi's ongoing studies.
NASA Goddard/A. Mellinger, CMU; T. Linden, Univ. of Chicago

IC 443, the Jellyfish Nebula

The shock waves of supernova remnants like the Jellyfish Nebula can accelerate protons to near the speed of light. When they slam into nearby gas clouds, gamma rays are produced. Fermi detects this emission, confirming that supernova remnants accelerate high-energy cosmic rays. *NASA/DOE/Fermi LAT Collaboration/NOAO/AURA/NSF, JPL-Caltech/NASA*

LAT science

- LAT detected 5787 sources during the first 10 years
  - Released in the LAT 10-year point source catalog (4FGL-DR2)
- Catalog is constructed using “seeds” from catalogs at other wavelengths

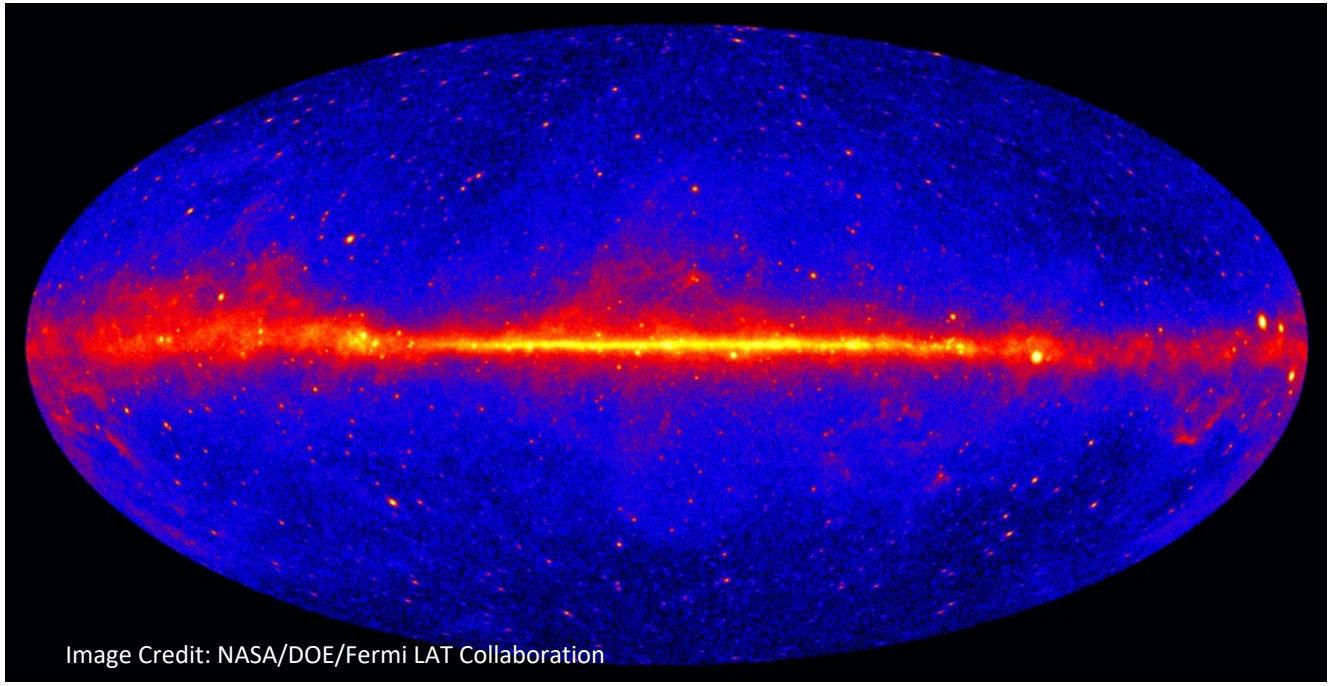

4FGL sources

- > 3100 Active galactic nuclei
- 232 Pulsars (most numerous Galactic source class)
- Pulsar wind nebulae, Supernova remnants, globular clusters, star-forming region, binary systems, novae, starburst galaxies, normal galaxies
- > 1300 Unidentified sources!

The Astrophysical Journal Supplement Series, 247:33 (37pp), 2020 March

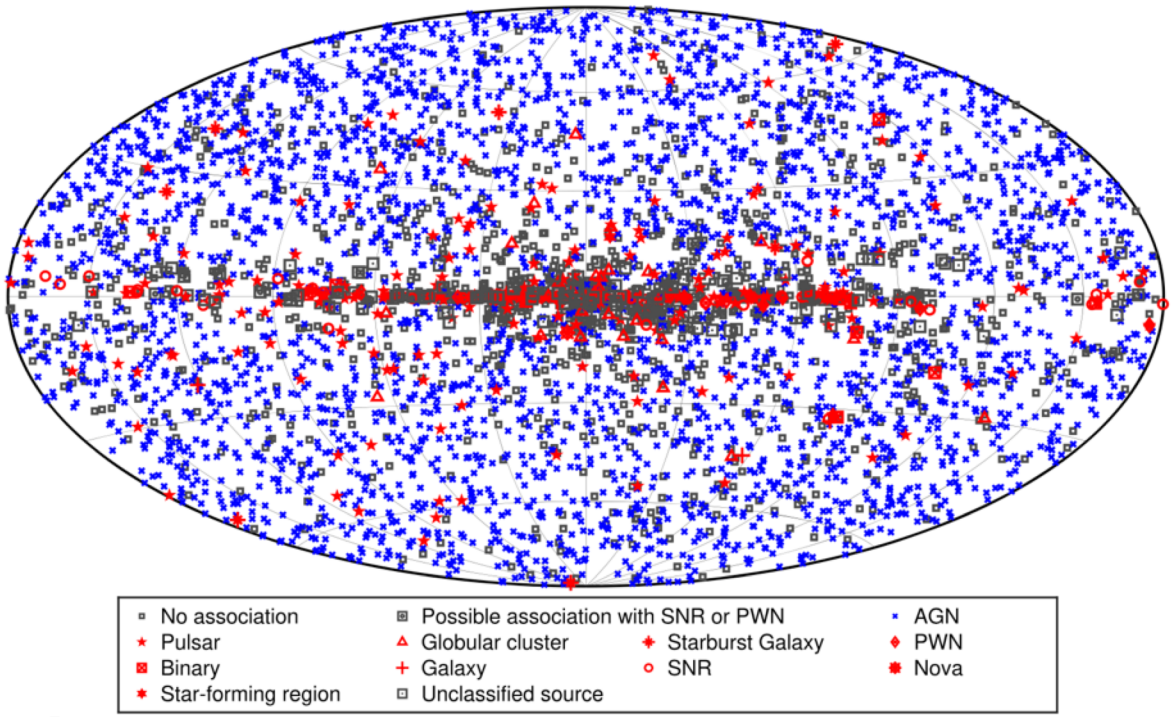

LAT vs. EGRET

EGRET detection

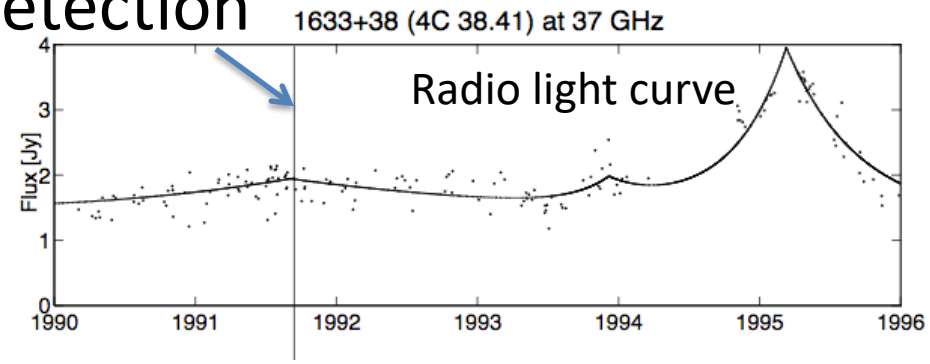

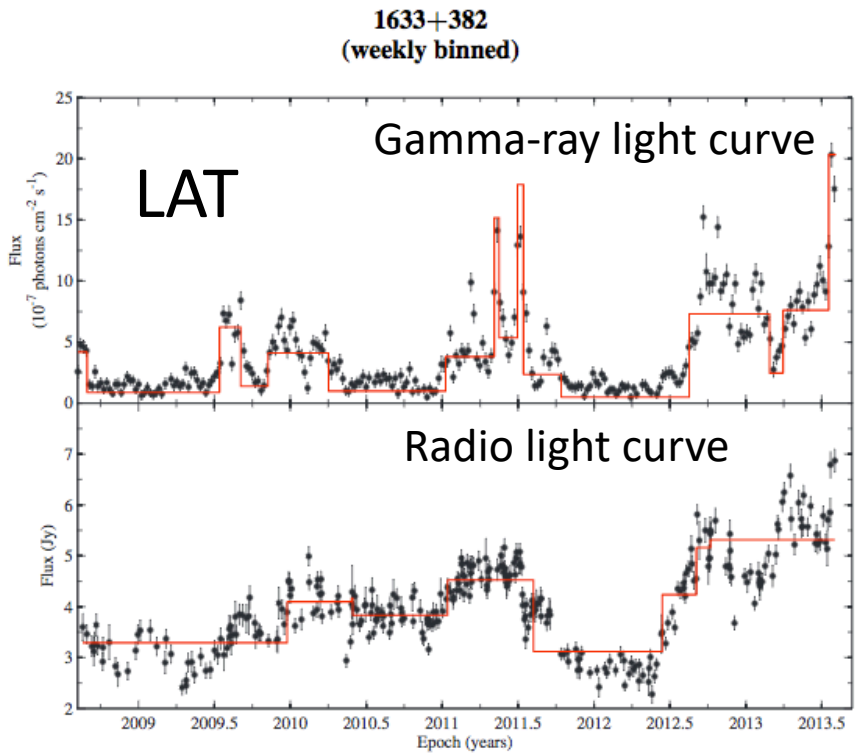

- EGRET did pointed observations
- EGRET could only determine if there were gamma-ray photons and their energy

- LAT has large field of view, all sources looked at every 3 hours
- LAT can see the variations in the gamma-ray photon flux

Dark Matter

- 27% of the Universe consists of so called dark matter, which does not interact with electromagnetic radiation
- Some of these weakly interacting massive particles (WIMPs) may produce gamma-rays through annihilation (opposite of pair production)
- Fermi sees an excess of emission in the Galactic center, which is consistent with simple dark matter models
  - Must be confirmed with more direct observations!

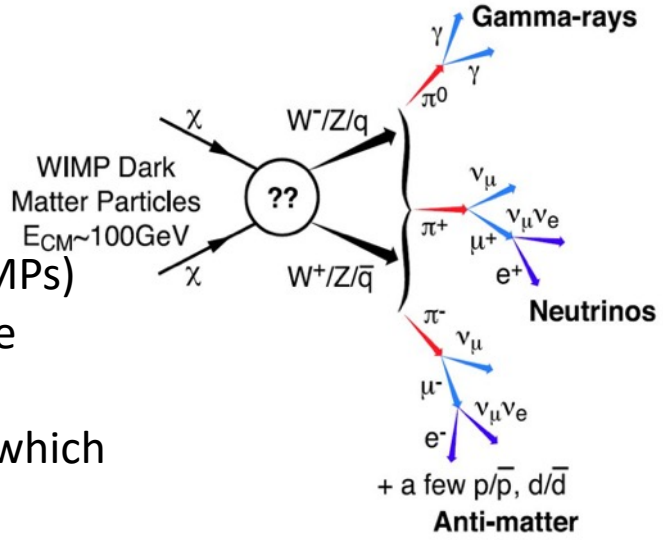

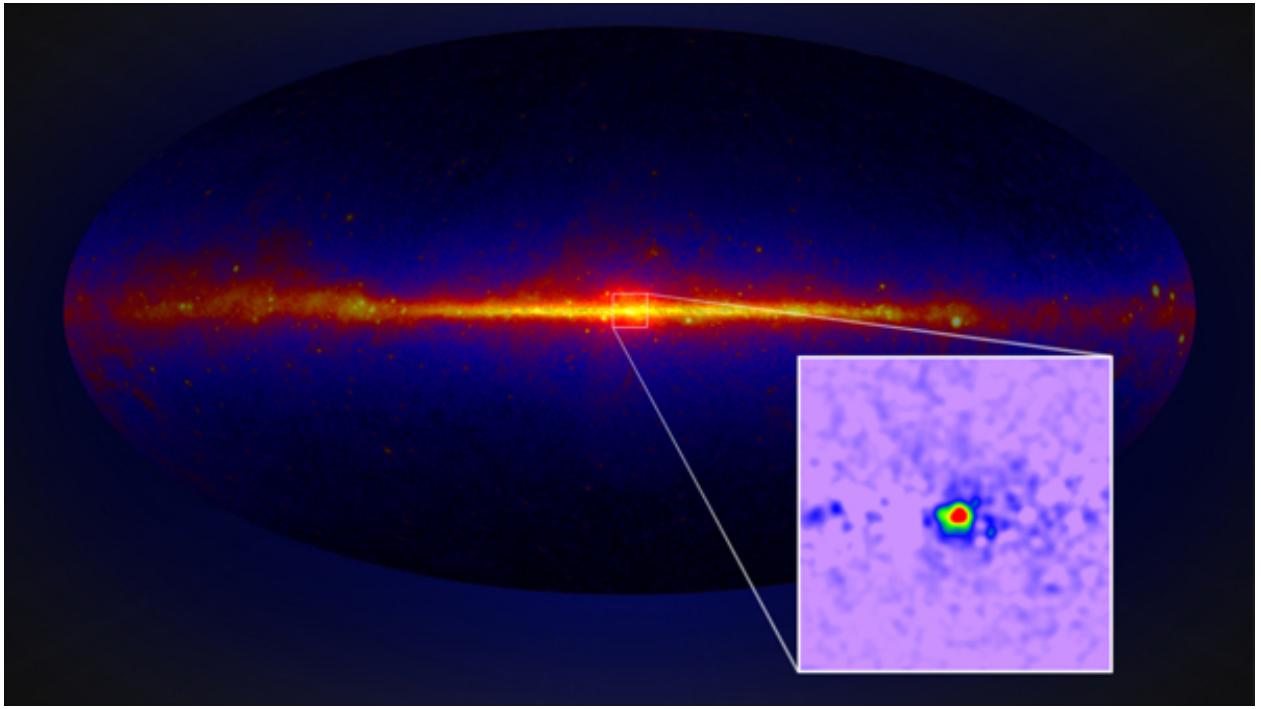

Electromagnetic counterpart to a gravitational wave event: Neutron star merger

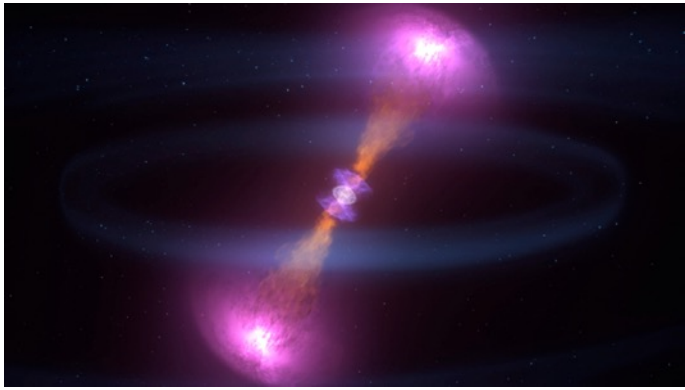

Fermi

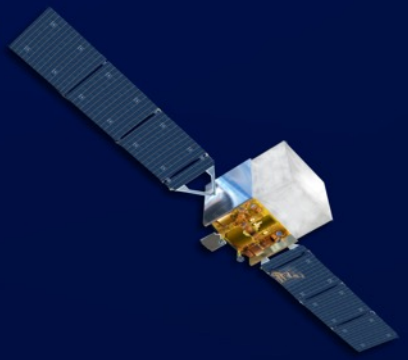

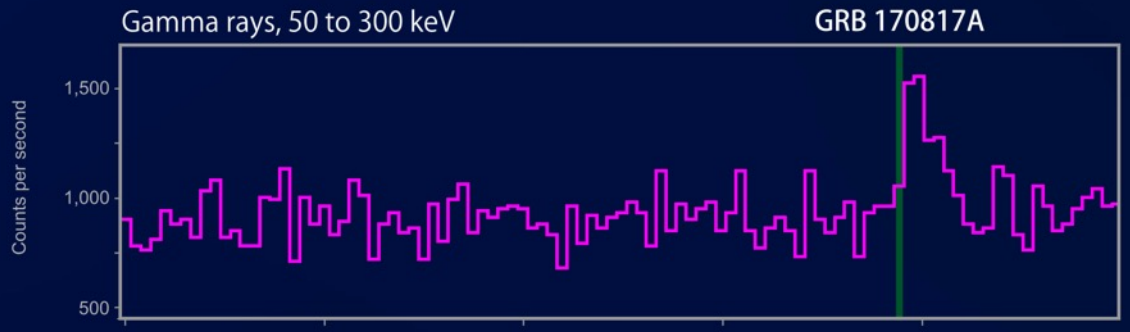

LIGO

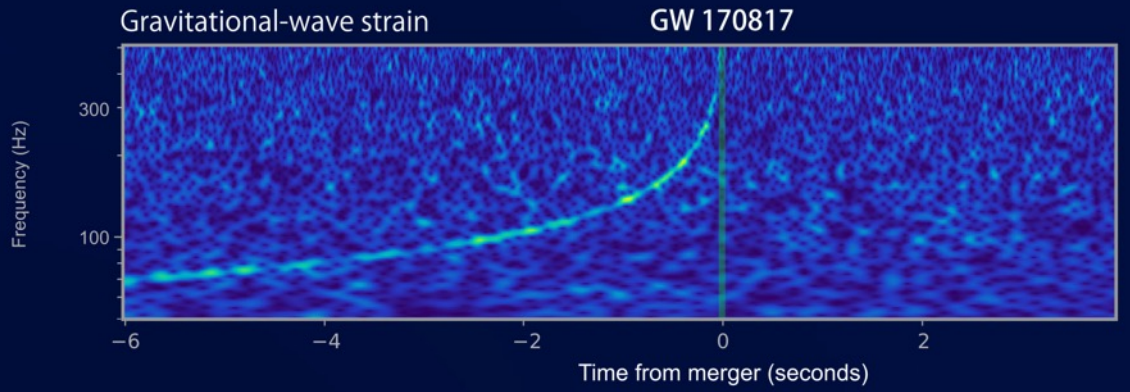

Fermi data analysis

- Data are sent down daily and are immediately available for user's to analyze
  - No proprietary period after the first year
  - Allows fast follow-up at other wavelengths for transient / varying objects
- Fermi Science Support Center provides tools and instructions on how to analyze the data
  - Fermi Science Tools
  - Analysis threads
  - > Allows even non-experts to analyze Fermi data

References and further reading

- C. Grupen, I. Buvat (eds.), Handbook of Particle Detection and Imaging
- Ackermann et al. 2012: Description of LAT and the instrument response functions (based on in-flight data)

http://iopscience.iop.org/article/10.1088/0067-0049/203/1/4/pdf

- Atwood et al. 2009: Description of the LAT instrument

http://iopscience.iop.org/article/10.1088/0004-637X/697/2/1071/pdf

- 4th LAT point source catalog (4FGL): LAT science

https://arxiv.org/pdf/1902.10045

- Fermi science tools: https://fermi.gsfc.nasa.gov/ssc/data/analysis/